

ANALYSIS OF BREAKDOWN IN POLLUTED INSULATOR USING NEURAL NETWORK MODEL

A DISSERTATION

*Submitted in partial fulfillment of the
requirements for the award of the degree*

of

MASTER OF TECHNOLOGY

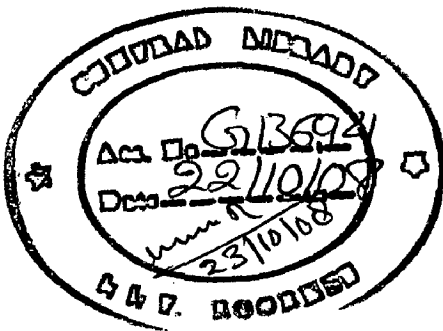
in

ELECTRICAL ENGINEERING

(With Specialization in Power System Engineering)

By

RAMDHAN SAHU



**DEPARTMENT OF ELECTRICAL ENGINEERING
INDIAN INSTITUTE OF TECHNOLOGY ROORKEE
ROORKEE - 247 667 (INDIA)
JUNE, 2008**

CANDIDATE'S DECLARATION

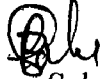
As partial fulfillment of the requirements for the Master of Technology (Electrical) Degree (Honors), I hereby submit for your considerations this thesis entitled:

“Analysis of Breakdown in Polluted Insulator Using Neural Network Model”

I declare that the work submitted in this thesis is to the best of my knowledge and ability and is an authentic record of my own work carried out during the period from July 2006 to June 2008 under the supervision of **Dr. E.Fernandez**, Assistant Professor, Electrical Engineering Department, Indian Institute of Technology Roorkee.

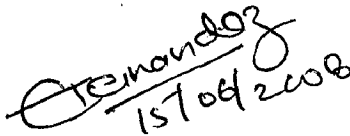
This work has not been previously submitted for a degree at the Indian Institute of Technology Roorkee or any other institutes.

Roorkee
Date: 12-06-08


Ramdhan Sahu
(Enroll. No 054017)

CERTIFICATE

This is to certify that the above statements made by the student are correct to the best of my knowledge.


15/06/2008
(Dr. E.Fernandez)
Assistant Professor,
Electrical Engg Department,
IIT Roorkee.

ACKNOWLEDGEMENTS

First and foremost, I would like to express my sincere appreciation to my thesis supervisors, Dr. E.Fernandez, for his patience and guidance throughout the entire duration of my thesis. Without his supervision, this thesis would never be a success.

I would like to express my deep sense of thankfulness to Prof. S.P. Gupta, Head of the department and Prof. J. D. Sharma, PSE Group Leader, for providing me better facilities to carry out this work.

I would like to take this opportunity to express my deep sense of gratitude to my family for their support and encouragement they have provided me over the years.

Last but not least, I would also like to thank my friends who have offered me their unrelenting assistance throughout the course.


(Ramdhan Sahu)

ABSTRACT

Electrical energy is generated at a distance from load centre and to minimize losses on transmission line; it has to be transmitted at high voltages. One of the faults that exist in high voltage insulator is the pollution flashover and subsequent outage of transmission lines. Since outage of EHV lines is a serious matter, research on pollution flashover invites concern.

Flashover on polluted insulator can occur when the surface is wet due to fog, dew or rain. Most commonly seen pollution related problem to flashover exist in coastal areas (sea salt), industrial areas (chemical pollution), and other areas (desert sands, etc.)

In the present dissertation, an attempt is made to develop suitable *ANN* models for predicting the flashover voltage (FOV) of contaminated insulators. The *ANN* models developed make use of the above three control (input) namely: salinity of contaminated salt, solution current and resistivity of salt solution. The output variable is the Flash over voltage (FOV). Since different architectures are possible, it is a voluminous task to explore all possible structures. Therefore, the study is restricted to the investigation of a few selected architectures, and the best ANN model from these is selected for subsequent simulation studies.

LIST OF FIGURES

Figure 1.1: Formation of Dry Bands on polluted surface	3
Figure 1.2: A partially damaged bushing due to pollution flashover	5
Figure 3.1: Type “A” insulator	12
Figure 3.2: Type “B” Insulator	13
Figure 3.3: Distribution of equivalent NaCl surfaces density along a path on the surface of type “B” insulator after tow year exposure in the desert	13
Figure 3.4: Type “D” Insulator	14
Figure 3.5: Distribution of equivalent NaCl surfaces density along a path on the surface of type “D” insulator after tow year exposure in the desert	14
Figure 3.6: Type “C” Insulator	15
Figure 3.7: Type “E” Insulator	15
Figure 3.8: Flashover voltage per unit suspension length, kV/cm Versus Exposure period in months	16
Figure 4.1: Details of Flat Plate Model	25
Figure 4.2: Configuration of the model	28
Figure 4.3: Dependence of V_{cx} on arc length	29
Figure 5.1 Model of neuron	33
Figure 5.2(a): Logistic function	34
Figure 5.2(b): Hyperbolic tangent function	34
Figure 5.3: Feedback in network	35

Figure 5.4: Kohonen Network	37
Figure 5.6: Signal- flow graph of the error back-propagation algorithm	42
Figure 6.2: Layout of Model A	47
Figure 6.3: Training Curve for Model A	48
Figure 6.4: Layout of Model B	48
Figure 6.5: Training Curve for Model B	49
Figure 6.6: Layout of Model C	49
Figure 6.7: Training Curve for Model C	50
Figure 6.8: Layout of Model D	50
Figure 6.9: Training Curve for Model D	51
Figure 6.10: Layout of Model E	51
Figure 6.11: Training Curve for Model E	52
Figure 6.12: Layout of Model F	52
Figure 6.13: Training Curve for Model F	53
Figure 6.14: Layout of Model G	53
Figure 6.15: Training Curve for Model G	54
Figure 6.16: Layout of Model H	54
Figure 6.17: Training Curve for Model H	55
Figure 6.18: Layout of Model I	55
Figure 6.19: Training Curve for Model I	56
Figure 6.20: Layout of Model J	56
Figure 6.21: Training Curve for Model J	57
Figure 6.22: Graphical Validation of Accuracy of ANN Model A	59

LIST OF TABLES

Table no. 3.1 Summary of Test Results	19
Table 3.2: Required conductivity of the Suspension	20
Table 6.1 ANN Models Configuration	46
Table 6.2 Summary of Training Results	58
Table 6.3 Analytical Values of FOV Obtains Using Model A	59

CONTENTS

Candidate's Declaration	ii
Acknowledgement	iii
Abstract	iv
List of figures	v
List of Tables	vii
1. Introduction	1
1.1 General	1
1.2 Why Pollution Flashover occurs	1
1.3 Mechanism of Pollution Flashover	2
2. Literature Review	6
3. Tests on Contaminated Insulators	10
3.1 Test on Contaminated insulator	10
3.2 Necessity of Test	10
3.3 Types of Tests	11
3.4 Test on insulator exposed to natural desert condition	11
3.4.1 Nature of the contaminant	11
3.4.2 Distribution of the layer	12
3.4.3 Flashover characteristics	15
3.5 Solid layer pollution deposit test	17

3.6 Salt fog test	18
3.7 Summary of Results of Salt Fog Tests	19
3.8 Solid layer Artificial Pollution Test	19
3.8.1 Basis of the test procedure	19
3.8.2 Cleaning	20
3.8.3 Application of the pollution layer	20
3.8.4 Wetting of the pollution layer	20
3.8.5 Determination of the layer conductivity	21
4. Theories of Flashover in Polluted Insulator	22
4.1 Introduction	22
4.2 Flat Plate Models	23
4.3 Cylindrical Models	27
4.4 Summary	29
5. Artificial Neural Network an overview	31
5.1 Introduction	31
5.2 Properties of Artificial Neural Networks	32
5.3 The Model of a Neuron	33
5.4 Learning Processes	34
5.4.1 Error-Correction Learning	35
5.4.2 Memory-Based Learning	36
5.4.3 <i>Hebbian</i> Learning	36
5.4.4 Competitive Learning	37

5.4.5 Boltzmann Learning	38
5.5 Kohonen Self Organizing Network	39
5.6 Multilayer Perceptron	40
5.6.1 Introduction	40
5.6.2 Error Back-Propagation Algorithm	41
5.6.3 Achieving Better Performance	42
5.6.4 Improving Generalization	43
6. Artificial Neural Network Model for Flashover Voltage(FOV) Estimation	45
6.1 Introduction	45
6.2 The Control Variables	45
6.3 Activation Functions	45
6.4 ANN Architecture	46
6.5 ANN Models Developed	47
6.6 Software Used	47
6.7 Results and Discussion	47
6.7.1 Model Architecture/Configuration and Training	47
6.7.1.1 Model A	47
6.7.1.2 Model B	48
6.7.1.3 Model C	49
6.7.1.4 Model D	50
6.7.1.5 Model E	51

6.7.1.6 Model F 52

6.7.1.7 Model G 53

6.7.1.8 Model H 54

6.7.1.9 Model I 55

6.7.1.10 Model J 56

6.7.2 Discussion on the Training Trends of ANN Models 57

6.8 Verification of Accuracy of ANN Model 58

6.9 Summary 60

7. Conclusion 61

7.1 Summary 61

7.2 Scope of Further Work 61

References 62

INTRODUCTION

1.1 General:

Electrical energy is generated at a distance from load centre and to minimize losses in the transmission line, it has to be transmitted at high voltages. One of the faults that exist in high voltage insulator is the pollution flashover and the subsequent outage of transmission lines. Since outage of EHV lines is a serious matter, research on pollution flashover invites concern.

Flashover on polluted insulator can occur when the surface is wet due to fog, dew or rain. Most commonly seen pollution related problem to flashover exist in coastal areas (sea salt), industrial areas (chemical pollution), and other areas (desert sands, etc.)

1.2 Why Pollution Flashover Occurs

Development of partial discharge on the insulator surface and propagation of these discharges over a period of time causes the leakage current to increase on the insulator surface which may result in a flashover. This occurs in three stages. These are the formation of electrolytic conductive film layer, the formation of dry band and the starting of pre discharges and propagation of pre discharge. The first two stages can occur frequently; however, the last stage does not occur as often as the others. In the case of cap-and pin porcelain insulator, usually dry bands initially occur near the cap or the pin of the HV voltage insulator, and when the voltage on a dry band exceeds the air withstand –voltage sparks occur. If this dry band is bridged by a partial discharge, voltage drops and other dry band are created and a discharge chain starts.

Regarding the pollution of the insulator in the desert, it has been generally concluded that: -

- a) The early morning dew in the desert represents a major source of wetting the insulators.
- b) Sand storms increase the pollution of the insulators severely, the worst conditions occurring when sand storms are accompanied or followed by high humidity, or by rainy or misty weather.
- c) Pollution layer accumulated under on insulator during sand storms can be of larger grain size and have higher salt content than those accumulated under normal desert weather. The sandstorm pollution is usually carried by strong winds from distant regions.

1.3 Mechanism of pollution flashover

The flashover process develops in the following stages:-

a) Surface contamination:-

Insulators operated in contaminated atmosphere collect pollutants which are deposited on the surface of insulator. Deposition of pollutants on insulator surface depends on many factors e.g. shape of insulator, nature of voltage i.e. ac or dc, location, angle of inclination of insulator, wind, rain etc. The performance of insulator itself is not altered significantly by the presence of dry contaminants because of electrical strength of dry polluted insulator is close to that for the clean insulator

b) Wetting process: -

When the polluted insulator becomes moist due to fog or rain, then the polluted layer becomes conductive. The process of moistening depends on wetting condition e.g. moisture absorption depending upon the nature of contaminant, temperature of surrounding, condensation mounting etc.

c) Dry band formation: -

Due the presence of conductive layer the electric field is greatly distorted along the pollutant surface. As is known, the voltage gradient needed to initiate spark over in air is about 30kv/cm. The average surface voltage gradient of an outdoor H.V. insulator is about 500kv/cm. Therefore, in order to initiate an arc on a polluted insulator surface, the voltage distribution must be highly non-uniform. Formation of dry band on a polluted flat plate surface takes place in the following steps as shown in Figure 1.

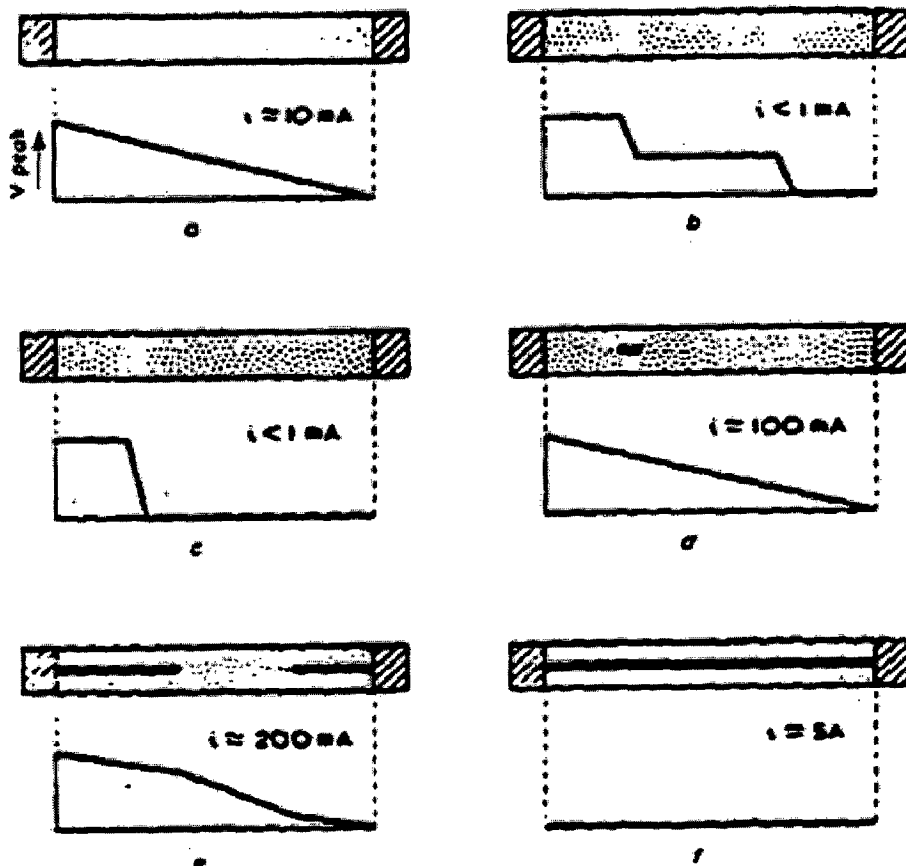


Figure 1: Formation of Dry Bands on polluted surface

Initially the plate is dry and then is then subjected to wetting. As shown in fig 1 “a” the voltage distribution is linear as resistivity of layer is uniform. As the layer becomes wet, its resistivity decreases and the surface leakage current increases. This condition does not last long

due to slightly higher resistance value in some location the voltage gradient in these location may exceeds that of air resulting in arc discharge root the area in the near vicinity of discharge dries out. The heat dissipation is more in these location and therefore the area dries more rapidly than remaining surface, forming dry band "b" If several dry bands are formed then after a short time only one dry band remains and due its high resistance nearly all the source voltage is dropped across this dry band as in fig "c" the width of the dry band changes until the voltage across it is just less than that required to initiate a discharge in air across it. Any moisture falling on the dry distort the electrical field in the band and discharge occur, a surge of the current is generated which dissipated the heat energy in discharge thereby drying band. The frequency of these surges, each of which may last for several cycles, is such that the mean power dissipated in the dry is just enough keeping it dry. After the formation of dry band a sudden increase in the applied voltage may lead to flashover of surface, while a gradual increase may cause dry band to widen. When this happen the arc extinguishes at current zero and restrikes. In the next half cycle in fig "d" and "e" and "f" indicate the condition several cycles after restrike. In figure "d" the voltage distribution is linear. During subsequent cycles the leakage current is increases and the arc lengthens and a greater portion of applied voltage appears across the rest of the polluted surface. A further dry band forms and flashes over immediately, as shown in figure "e" and finally, the separate discharge combine to span the entire polluted surface figure "f".

d) Breakdown of dry bands:- Almost the entire voltage appear across the dry band and when dry band can not sustain the voltage an arc is initiated and bridges the dry band

e). Propagation of arc: Depending on the applied condition e.g. applied voltage leakage

Current etc. the arc may be further and bridge the insulator surface resulting in flashover or it may extinguish prior to flashover.

Figure 2 shows a porcelain bushing that has been partially damaged by pollution flashover discharges.

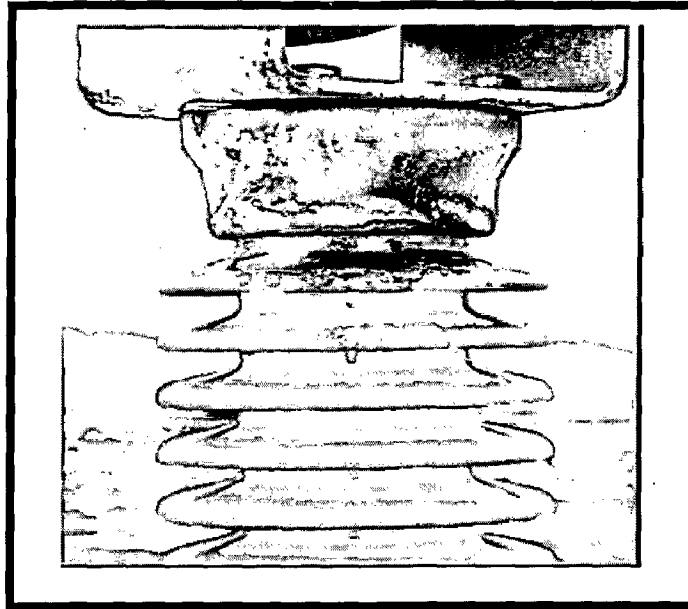


Figure 2: A partially damaged bushing due to pollution flashover

DC flashover voltage is lower than the AC, for the same operating conditions. Under dc voltage there is no current zero. More ever more pollutant are attracted to an insulator under DC voltage than due to AC. Also, due to absence of current zero the propagation of arc is easier in DC than in AC. The flashover voltage in ac and dc depends on many factors and even when experiment is conducted under the same controlled conditions, the flashover voltage may not be the same. This applies for both AC and DC.

LITERATURE REVIEW

Various investigators in relation to pollution flashover phenomenon have carried out in a number of research studies. Some of the several reports available in the literature are briefly presented as follows:

Farouk et al [1] presented a comparative analysis of the tests carried out on polluted insulators subjected to the desert environment in which the effect of sand deposits is predominant.

Abdel-Salam et al [2] conducted studies on flashovers observed under desert environmental conditions in insulators. They investigated the flashover characteristics for porcelain insulators exposed to natural sandstorms, as well as to simulated sandstorm with and without a charged grid. They showed that neither natural nor artificial sandstorms affect the fast flashover voltage if the sand particle is not charged, whereas charged particles of sands reduce the flashover voltage of the insulators. To a higher extent, this reduction in flashover voltage will be greater for DC voltages.

Prem K. Patni[3] presented a detailed review of various models that have been developed to explain pollution flashover.

W.Heise, G.F. Luxa, G.Revery and M.P. Verma [4] presented an assessment of a solid layer pollution test for flashover in polluted insulators.

Sundrarajan R. and Gorur R.S.,[5] presented their findings in relation to the role of non-soluble pollutants in the flashover mechanism They considered the effect of the shape of the insulator in determining the flashover voltage magnitude.

In another paper, the same authors [6] evolved a dynamic arc model to explain the flashover mechanism under DC conditions for polluted insulators

Raghuveer M.R. and E. Kuffel [7] conducted experimental and analytical studies of factors which affect pollution flashover voltage on polluted insulation surfaces.

In yet another paper, **Sundrarajan R. and Gorur R.S., [8]**. developed dynamic models to estimate the pollution flashover voltage for various practical insulator configurations. The dynamic models also computed flashover voltages of non-uniformly distributed insulators configurations, which is more representative of the service experience.

Zafer Aydogmus and Mehmet Cebeci, [9] presented a new flashover dynamic model of polluted Insulators”

Holzhausen J.P. and Swift D.A [10] developed theoretical models to predict the flashover on the practical cap and pin type insulators. They found that the arc constant varies with pollution severity and that this variation can be attributed to the arc across the dry bands not following the insulator surface, but taking shorter routes. This analysis is done for AC and DC energies cap and pin insulators by comparing the results obtained, using the appropriate theoretical model, with test data..

Obenaus F., [11] was the first to propose a quantitative analysis of the arc on a polluted surface. In his model, an arc is considered in series with the wet polluted layer having a resistance Based on this simple model and knowledge of arc voltage, the flashover voltage can be predicted.

Wilkins, R. [12] developed a formula for calculating the resistance of the polluted layer and factor which takes into account the change in resistance due heat are derived. Criteria for flashover i.e. $di/dx > 0$ is presented and applied to compare the experimental results. The model can be applied to axi-symmetric insulator with complex shape by replacing the practical insulator by its equivalent cylinder. For developing flashover criteria he s assumed that the discharge moves to a position where the rate of energy expenditure is maximum. A critical current value may be calculated above which power increased with the leakage discharge length and below which power decreased with discharge

length. For a discharge length of x , the movement will occur if $\frac{dp}{dx} > 0$. Where “p” is power taken from source.

Alliston L.L. and Zoledziowski, S.[13] proposed a theory that attempted to explain the growth of discharge phenomenon in contaminated insulator surfaces.

The above models made use of conventional methodologies of analysis. However, recently, there is a trend towards the application of artificial intelligence methods (mostly ANN's) for prediction of flashover voltages, Some of the recent work in this direction is discussed in the following accompanying studies:

Ahmad S. et al, [14] successfully applied artificial neural networks in pollution severity measurement studies for function estimation. Modeling of the complex non-linear function *ESDD* (which is a complex function of several variables), the equation of which is unknown, was accomplished accurately. Further comparative analysis of the estimated results with the measured data collected from the site measurement amply demonstrate the effectiveness of the use of ANN in modeling *ESDD* that has an unknown nonlinear relationship .the estimation of critical contamination level in terms of *ESDD* will help in fixing maintenance policy and addressing an effective solution against pollution flashover of high-voltage insulator.

Dixit and Gopal [15] did a study which attempted classify the transition from weak inception current flow on the surface of the contaminated porcelain insulators till flashover occurs. It was classified into three stages which can be explained in terms of arc voltage gradient. The more popular *Ayrton's* equation was chosen which computes arc voltage gradient in terms of arc current I and *Ayrton's* constants A and n . The present work describes the development of a multi layer *Feed Forward Neural Network (FFNN)* classifier model using back propagation algorithm for training, to discriminate the arc gradient for the three stages considered, for the

given values of A , n and I as the input parameters. The model is tested and the results show that, Neural Network structure with six nodes in the hidden layer is best suited for the present classification. The percentage of correct classification is found to be 100% in all the three classes.

Kontargyri et al [16] attempted to apply artificial neural networks to estimate the critical flashover voltage on polluted insulators. The artificial neural network used as input variables the following characteristics of the insulator: diameter, height, creepage distance, form factor and equivalent salt deposit density ($ESDD$), and estimated the critical flashover voltage. The data used to train the network and test its performance was derived from experimental measurements and a mathematical model. Various cases were studied and their results presented separately. Training and testing sets were modified for each case.

Ghosh, et al [17] carried out modeling of flashover characteristics of electrolyte contaminated surfaces using artificial neural networks.

Al-Alawi, et al [18] attempted the prediction of flashover voltages of contaminated insulators using artificial neural network. They used experimental data pertaining to the salinity and electrical characteristics of the contaminant solution

Tsanakas A.D. and Agoris D.P [19] presented an approach for forecasting the number and the location of faults, caused by pollution flashover in 15 KV overhead distribution network. Faults were forecasted with an expert system that combines forecast of different models of feed forward neural networks and neuro- fuzzy inference system.

Thus it may be seen from this brief review, that the subject of Pollution Flashover in polluted insulators is one of considerable research interest. The topic is still an active area of further research

TESTS ON CONTAMINATED INSULATORS

3.1 Test on contaminated insulator

To describe the performance of various type of insulator exposed to natural pollution condition, it is necessary to understand what types of test s are performed on the insulator. These tests include chemical and grain size analysis of the contaminant, layer distribution as well as flashover test of the naturally contaminated insulator wetted by clean fog.

3.2 Necessity of test

- 1). The test is necessary to determine the order of merit of the tested design. It will analyze the quantitative data concerning the effect of insulator profile on their performance under desert condition.
- 2). Flash over characteristic of the different strings is also indicated according to the dust deposit method
- 3).To calculate the withstand capacity at system phase voltage as well as the system flashover voltage at fixed salinity.
- 4).For comparing the result i.e. test performance and actual performance in natural condition.
- 5). Determination of the amount and distribution of foreign deposit material.

- 6). Dust deposit artificial test also produce the same order of merit as test on naturally polluted insulator although they did not reveal the particular of insulator behaviors in the same quantitative manner.
- 7). for determination of the layer conductivity.
- 8). for determination of withstand characteristic of insulator.

3.3 Types of tests The test may be classified into four categories:-

- A). Test on insulator exposed to natural desert condition.
- B). Solid layer deposit pollution tests.
- C). Salt fog tests.
- D). Solid layer artificial pollution test

3.4 Test on insulator exposed to natural desert condition

Insulator strings were suspended un-energized on a portal at a mean height of about 25m above ground level in a desert environment over a period of tow year. Insulator sample were dismantled for test purpose after 6-8 month, 12- 13 months and 24 months of exposure.

3.4.1 Nature of the contaminant

Chemical analysis of the natural contaminant showed that the soluble salts amount to 17.8%, mostly consisting of sulphates and chlorides $CaSO_4$: 9.92% NaCl 2.97% and KCl 0.53 by weight of the deposit.

Grain size analysis of contaminant reveals that 95% by weight of the material has grain dimension smaller than $44 \mu m$. For comparisons, the same analysis was carried out for a sample from the surface of the soil in the area. This showed that the above dimension of $44 \mu m$ and less is found in 0.15% only of the soil sample, while 88% of the sample consist of grain

dimension greater than $105 \mu\text{m}$. The overall salt content of the soil was determined at 0.4% only although for the particles with grain dimension of $44 \mu\text{m}$ and less the corresponding value is 1.36%.

3.4.2 Distribution of the layer

One objective of the testing is to investigate the effect of insulator shape on the amount and distribution of the contamination layer. As is usual with natural pollution the layer was found to be far from uniform on all the insulator types. Beside the non-uniformity of the layer along the leakage path there was also a lack of circular symmetry of the layer distribution. The effect of shape was particularly distinct in comparing the relative weight of the contaminant on the lower and upper surfaces of each insulator i.e. on the protected and unprotected areas respectively. For example, after 24 months of exposure the above ratio reached 18-20 for the ribbed insulators, type A and C, while it was occasionally as low as unity for the flat design type B.

Figures 3.1, 3.2 and 3.4 show the basic internal structures of ribbed insulators of types A, B & D, while Figures 3.3, 3.5 and 3.8 show the effect of contaminant on their respective breakdown voltages.

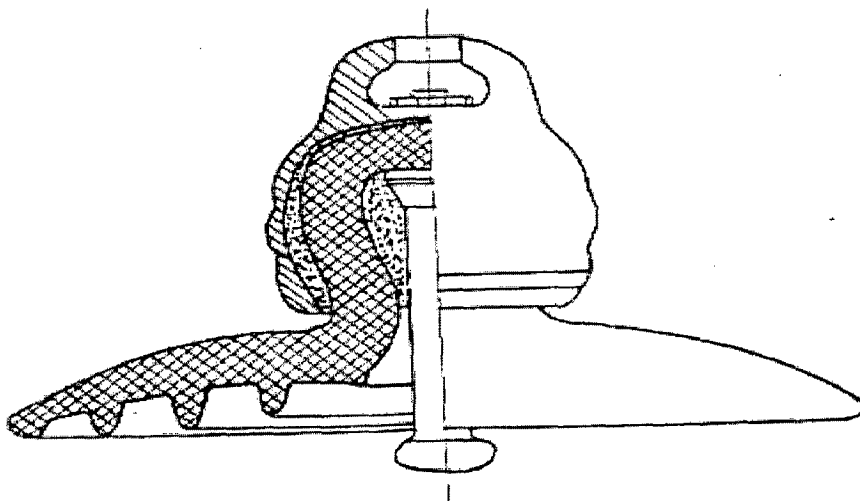


Figure 3.1: Type "A" insulator

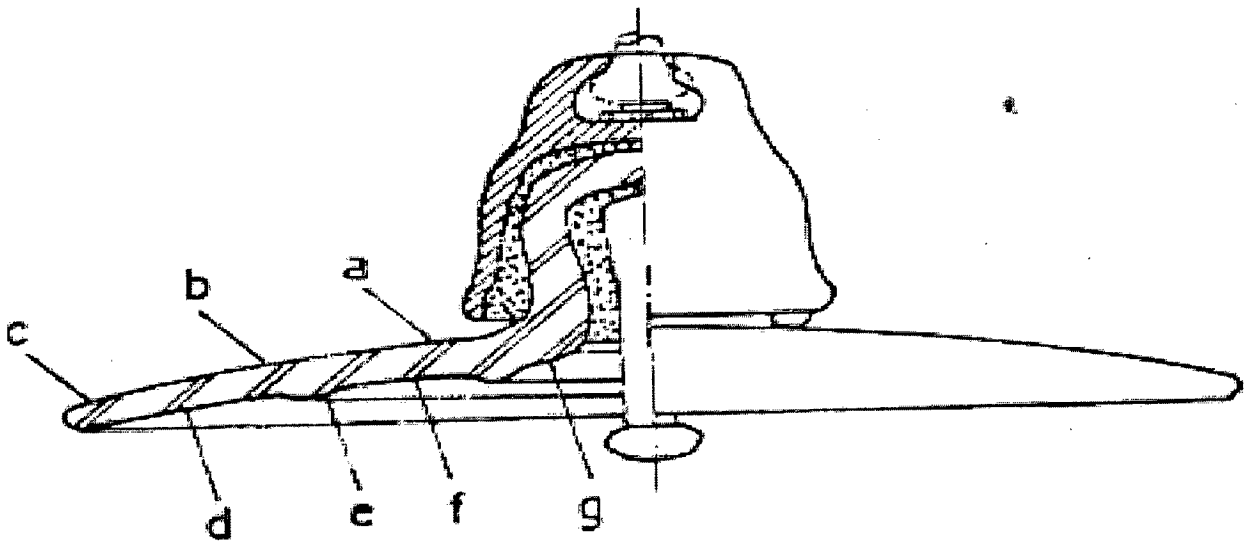


Figure 3.2: Type "B" Insulator

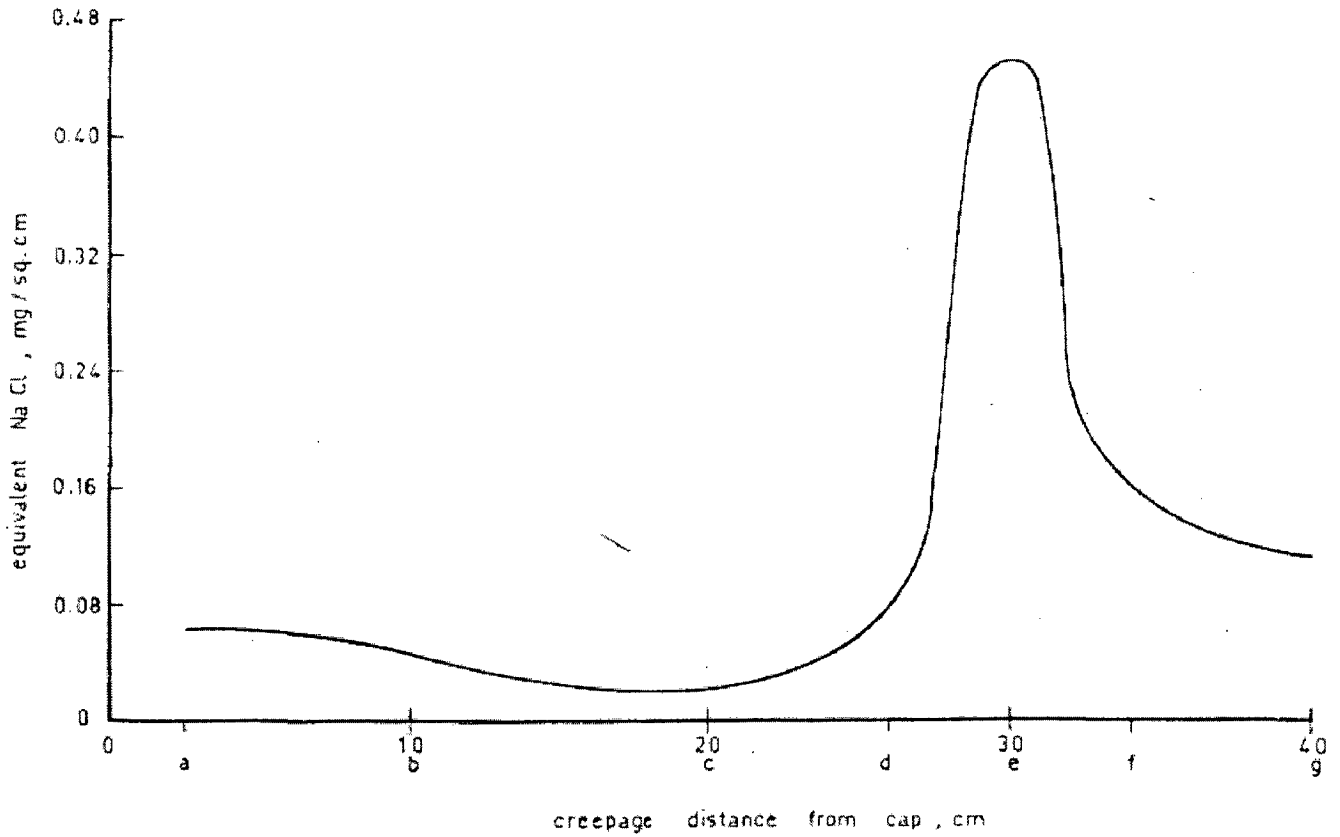


Figure 3.3 Distribution of equivalent NaCl surfaces density along a path on the surface of type "B" insulator after tow year exposure in the desert.

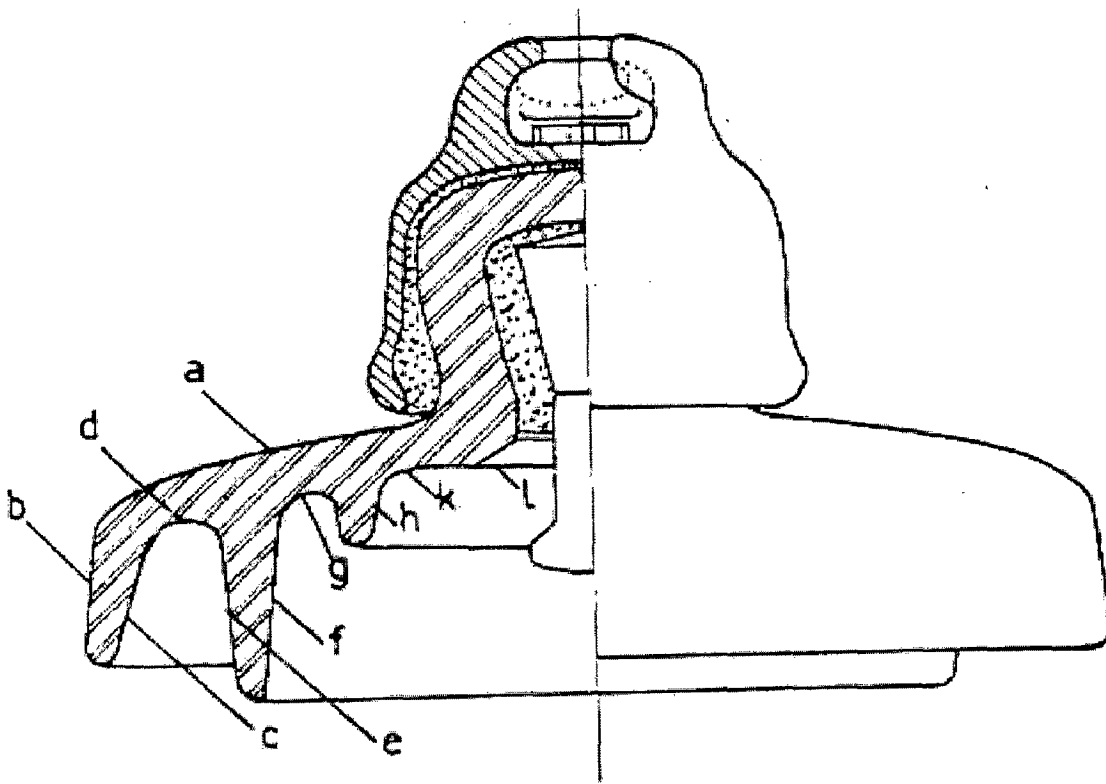


Figure 3.4: Type "D" Insulator

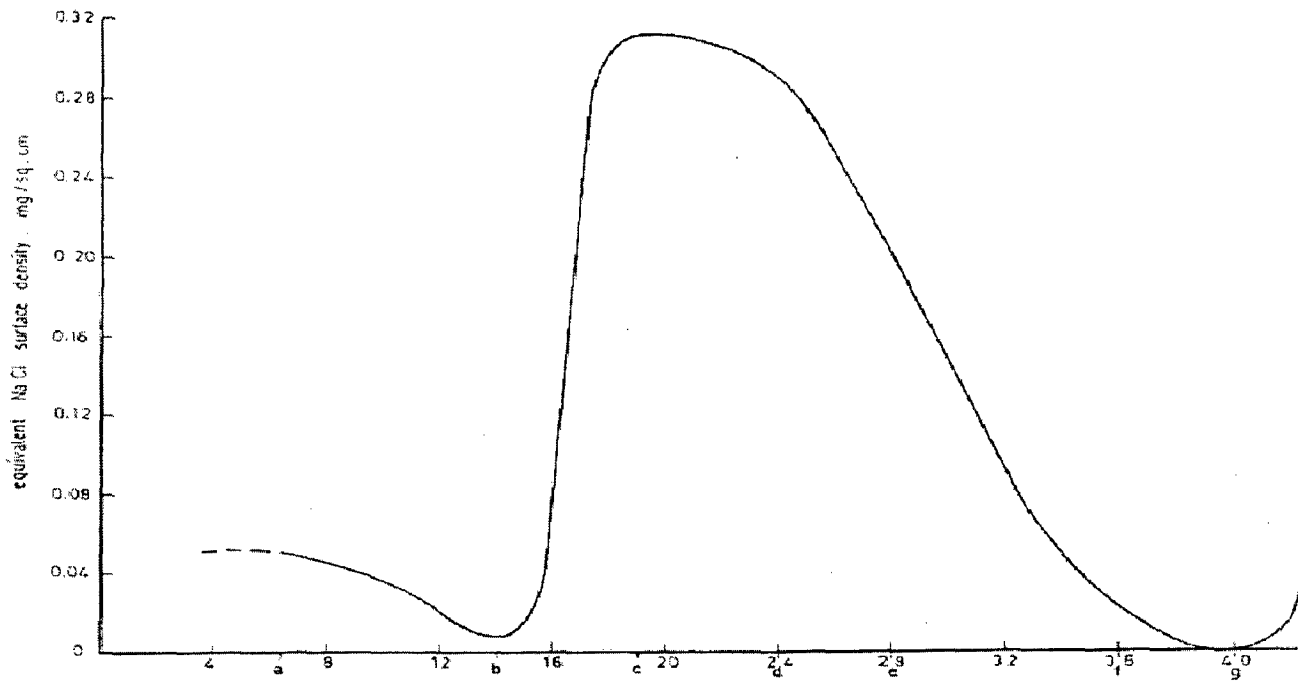


Figure 3.5: Distribution of equivalent NaCl surfaces density along a path on the surface of type "D" insulator after tow year exposure in the desert.

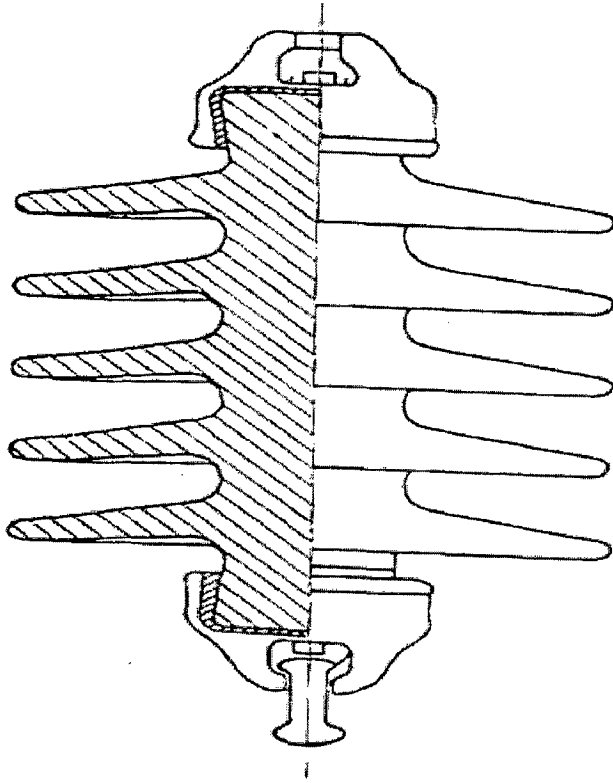


Figure 3.6: Type "C" Insulator



Figure 3.7: Type "E" Insulator

Figures 3.6 & 3.7 show the structures of Type C & Type E insulators.

A pollution monitor directly graded to read equivalent NaCl surface density was used to determine the distribution of the contaminant following paths along the insulators when saturated with clean fog. Two examples of such distributions after 24 months of exposure are shown in figures 6 & 8 for insulator type B and C respectively.

3.4.3 Flashover characteristics:

Beside the amount and distribution of the foreign layer the insulator shape in itself has, of course, a major influence in determining the flashover voltage. Flashover test were carried out there fore on the different insulator types after different periods of exposure to natural pollution. Wetting took place by clean fog under constant applied voltage, and test was repeated on similarly polluted insulator with the voltage changed according to the staircase method. For space limitation only a summary of the result could be reported here. The result of flashover tests are shown in figure where, for the sake of comparison, they are expressed in terms of the

flashover voltage per unit suspension length of each insulator type. This quantity is adopted as the measure for the order of merit of each design. After one year of exposure, with a total rain intensity amounting to 2.8mm, the favorable effects of the flat design from the point of view of self-cleaning by wind were quite apparent. The specific flashover voltage per unit creep age length was found to be 368V/cm and 329V/cm for type B and C respectively as compared to 239V/cm for the deep-ribbed type A and C respectively. On the other Than, the relatively high ratio of leakage length to spacing of type D insulators, proved quite favorable as clearly shown by figure the second year of exposure, although obviously a dry year, brought the much heavier rainfall of 14.9mm. On one day during the 19th month of exposure the rain fall amounted to 7.6 mm and on another day during the 22nd month there was 4.4mm of rain.

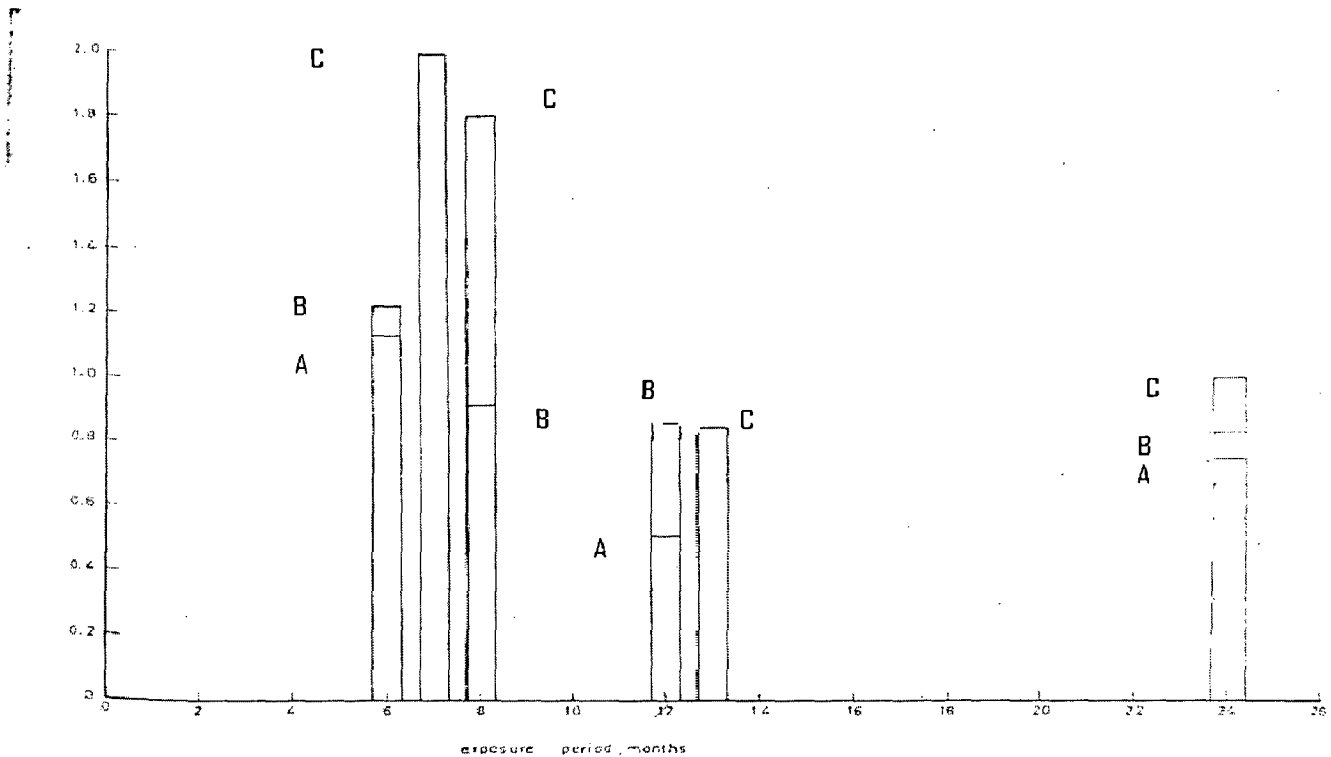


**Figure 3.8: Flashover voltage per unit suspension length, kV/cm
Versus Exposure period in months**

Judging from the ratio of shed overhang to shed spacing, it is found that for type A insulator this ratio is much in excess of the corresponding values of the other designs. It is believed therefore

that type A was the least cleaned by rainfall and that this is the reason for the relative deterioration of its performance in the tests at the end of the second year. If the order of merit is determined according to the lowest specific flashover voltage per unit suspension length reached during the two years of exposure, then insulator C assume the first rank followed by B, and A.

3.5 Solid layer pollution deposit test

These tests are performed on strings of almost equal suspension length consisting of 7 discs of insulator types A, B, D, 3 insulator of type C and one insulator type E. In this way, the string lengths are in the range of 127(+/-) 8 cm. The test procedure is not described here, only the results are discussed. The results are shown in figure it is noticed that for the range of heavy pollution, the order of merit starting with the best insulator is D, B, C, A and E which is identical to that determine from test on naturally polluted insulators reported above. It should be noticed however, that in the range of heavy pollution, the dust deposit tests show only minor differences between types B, C and A. This is contrary to clear superiority of type B over type A as revealed by natural tests. Another point is that for the present case of uniform artificial pollution the performance of type D insulator compared to those of B, C somewhat deteriorated in the vicinity of $10 \mu s$. An explanation may be that for that deep ribbed type, the leakage path is not fully utilized at lighter pollution I.e. some of the ribs are over bridged by the arcs without following the insulator profile.

Presentation of the results on logarithmic paper showed that a reasonably close fit of the relationship between the 50% flashover voltage \bar{U} and the specific layer conductivity χ_s is given by:

$$\bar{U} = \alpha \chi_s^{-\beta}$$

Where, α And β are constants for each insulator type. The exponent β for the insulator type A, B, and C were found to be 0.39 0.40 and 0.36 respectively. It is interesting to note that from a simplified theoretical flashover criterion under alternating voltage this exponent was deduced as 0.40.

The test result showed that for all the insulator types investigated there was a tendency of decreased relative dispersions of the flashover voltage: , with heavier pollution. So while at $10 \mu s$ the value of σ / \bar{U} were in the range of 10-17%, the corresponding range at $40 \mu s$ was 4-8%.

3.6 Salt fog test

Salt fog tests are also carried out on the 110kv sting of different designs described above In one such test, the tested insulators consisted of 7 insulators of type A, B,& D, 3 insulators of type C and one insulator of type E per string. The spraying system and the testing procedure to obtain the withstand salinity at the system phase voltage of 63.5kv was in conformity with the concentration of the salt solution used in the tests was adjusted to one of the values:

5-7-10-14-20-23.8-28.0-33.6-40.0-47.5-56.5-80.0-112-160-224kg/mm².

(With proper correction of solution conductivity to 20 degrees Centigrade.)

Also average flashover voltage of the above strings at a fixed salinity, here chosen as 33.6kg/ m³ , was determined following, to a large extent, a procedure described in briefly below:

The insulator was energized at 90% of its estimated flashover voltage for minutes during the build-up of the saline fog.

The voltage was then raised in 5kv steps (6-10%) in five minutes intervals until flashover. The insulator was re-energized at 90%of this flashover voltage for 5 minutes and the voltage was then raised in steps of 2.5kv (3-5%) every 5 minutes until flashover.

This last test is repeated four times and the average of all the results except the first is taken as the mean flashover voltage.

3.7 Summary of Results of Salt Fog Tests

Table 3.1 shows the test results of the described tests carried out on the insulators:

Table 3.1 Summary of Test Results

String type	Withstand salinity at 63.5kV,g/l	Average F.O.V., KV at 33.6 g/l salinity	Order of merit
A	28	69	3
B	14	60	4
C	40	71	2
D	47.5	86	1
E	7	49	5

This order of merit however is different from those obtained from the dust deposit test and from the test of insulator exposed to natural desert pollution, as described above.

The table shows the relationship between the average flashover voltage at fixed salinity of 33.6 g/l and the leakage path length for the different strings, confirming the fundamental importance of this quantity to insulator performance under pollution conditions. The comparison of the individual results with the regression line determined by the least square method reveals the favorable effects of the deep ribs of types D and A under this test. On the other hand the flat aerodynamic profiles of insulator types B and C appear less suited to salt fog condition.

3.8 Solid layer Artificial Pollution Test

3.8.1 Basis of the Test procedure:-

For the solid layer test a layer consisting of a solid material with ion-building ingredient is applied on the surface of the insulator. Wetting makes this layer conductive.

3.8.2 Cleaning

The insulator shall be care fully cleaned with a detergent in order to remove all traces of grease. Hereafter the insulator surface shall be rinsed with mains water of low conductivity ($<500 \mu \text{ s/cm}$).the surface of the insulator is deemed to be sufficiently cleaned and free from any grease, if large continuous wet areas observed.

3.8.3 Application of the pollution layer:

A suspension of the following composition shall be used for application of the layer on the surface of the insulator:

100 g *kieselguhr* (diatomaceous earth, diatomite)

10 g aerosol (silicon dioxide of particle size 2-20 $\mu \text{ m}$)

1000 g water

The conductivity of this suspension shall be adjusted by adding a suitable amount of salt to obtain corresponding layer conductivity according to Table3.2

Table 3.2: Required conductivity of the Suspension

Layer conductivity with wetting at $\pm 20^\circ \text{ c}$ in $\mu \text{ s}$ (tolerance: $\pm 15\%$)	5	10	20	40
Correspondence conductivity value of the suspension at 20° c in $\mu \text{ s/cm}$	1500	3000	χ_r 6000	12000

Suspension should be applied on the clean and dry surface of the insulator by means of one or several atomizing nozzle to obtain a reasonably uniform layer.

3.8.4 Wetting of the pollution layer:

The polluted insulator shall be installed in the test chamber in its test position. Hereafter the insulator shall be Wetted with steam fog uniformly over its whole length. The temperature of the

test shall not exceed 40°. The intensity of wetting shall be so adjusted that the highest wetting of the layer and consequently the highest layer conductivity is reached in about 15 to 20 minutes. For this a rate of flow of approximately 0.7-kg/hour steam per cubic meter chamber's volume is necessary. During wetting of the pollution layer no dripping of moisture shall take place.

3.8.5 Determination of the layer conductivity:

During the wetting of insulator, the leakage current shall be repeatedly measured; the voltage applied only for long enough to read the meter. The alternating measuring voltage shall be about 2kv R.M.S. per meter of the flashover distance of the insulator. The highest layer conductance, determined out of voltage-current measurements, shall be multiplied by form factor f of the insulator giving the layer conductivity χ_p .

The form factor shall be determined from the insulator dimension. For graphical estimation of the form factor, the reciprocal value of the insulator circumference ($1/b$) is drawn against the leakage paths. The form-factor is given by the area under this curve and is calculated accordingly.

THEORIES OF FLASHOVER IN POLLUTED INSULATORS

4.1 Introduction

Flashover on transmission line insulation due to pollution insulator was reported as early as 1902. Since then, an appreciable number of experimental and theoretical studies have been conducted to understand the complex process of insulator flashover. The flashover process mainly involves the propagation of arc on a polluted surface. For an arc to propagate two conditions must be satisfied. These conditions are:

- 1). Electrical condition initiation and maintaining the arc (i.e. applied voltage and current)
- and 2) mechanism involving force which is responsible for movement of the arc generated from condition "1".

Despite considerable research work, the processes involved in flashover are still not fully understood. Studies were aimed to find the necessary conditions for initiation of an arc and then elongation of the arc. The process of flashover depends on factors such as type and nature of pollutant, non-uniform wetting process, conductivity of wet layer, orientation, shape and profile of insulator, wind, location, etc. Therefore the researchers faced a formidable task to find a suitable solution, which will take into account the effects of all the factors.

Based on experimental and theoretical studies many models were presented to explain the process of flashover. Since it is impossible to account all the factors involved, therefore the researchers had to make some assumptions in developing these models. It is therefore not

surprising to come across different theories explaining flashover mechanism. It is desirable to compare some important models to predict the flashover voltage

An overview of various theories /models which explaining to pollution flashover: is presented as follows:

4.2 Flat Plate Models

[A] **Model of F. Obenaus:** - Obenaus was first proposed a quantitative analysis of the arc on a polluted surface. In this model an arc of length “x” is considered in series with the wet polluted layer having a resistance “Rp”. Based on this simple model and knowledge of arc voltage, the formulae for calculating the minimum voltage required to sustain an arc has been derived, which is given below:-

$$V_{cx} = \frac{n+1}{n^{(n+1)}} N^{\frac{1}{(n+1)}} x^{\frac{1}{(n+1)}} R_p^{\frac{n}{(n+1)}}$$

Where,

V=applied voltage

X= arc length

I=leakage current

$R_p = R_p$ pollution resistance

n= exponent of static arc characteristics

N=static arc constant

- In this model assume that flashover occurs if the discharge is able to bridge the insulator without extinguishing.
- This model was developed for dc voltage.

- In this model identifies the necessary condition for flashover but not the sufficient condition. This means that it identifies the voltage, below which no flashover can occur due to discharge extinction, but not higher value at which the flashover will occur.

[B] Model of G. Neumarker

The model of Obenaus was applied by Neumarker with one difference. Instead of considering a fixed resistance of pollution layer in series with arc, Neumarker considered a uniform resistance per unit length of wet polluted layer. In this model the formula relating the minimum voltage required an arc and x/L are derived, where L is length of polluted surface. Also an equation for the critical arc length is derived.

Equation for critical flashover voltage is given below:-

$$V_{cx} = \left[\frac{r_p}{nN} \left\{ \left(\frac{x}{L} \right)^{\frac{1}{n}} - \left(\frac{x}{L} \right)^{\frac{n+1}{n}} \right\} \right]^{NL(1+n)}$$

X_c = Critical arc length

This model is applicable to DC voltage and could be valid under AC energization by considering ac as series of application of fixed voltage equal to that peak alternating voltage.

[C] Model of R. Wilkins

In this model formula for calculating the resistance of the polluted layer and factor which takes into account the change in resistance due heat are derived. Criteria for flashover i.e. $di/dx > 0$ is presented and applied to compare the experimental results. The model can be applied to axi-symmetric insulator with complex shape by replacing the practical insulator

by its equivalent cylinder. For developing flashover criteria he was assumed that the discharge moves to position where the rate of energy expenditure is maximum. A critical current value may be calculated above which power increased with the leakage discharge length and below which power decreased with discharge length. For a discharge length of x , the movement will occur if

$$\frac{dp}{dx} > 0. \text{ Where "p" is power taken from source.}$$

The flat plate model and discharge are shown in Fig 4.1 below

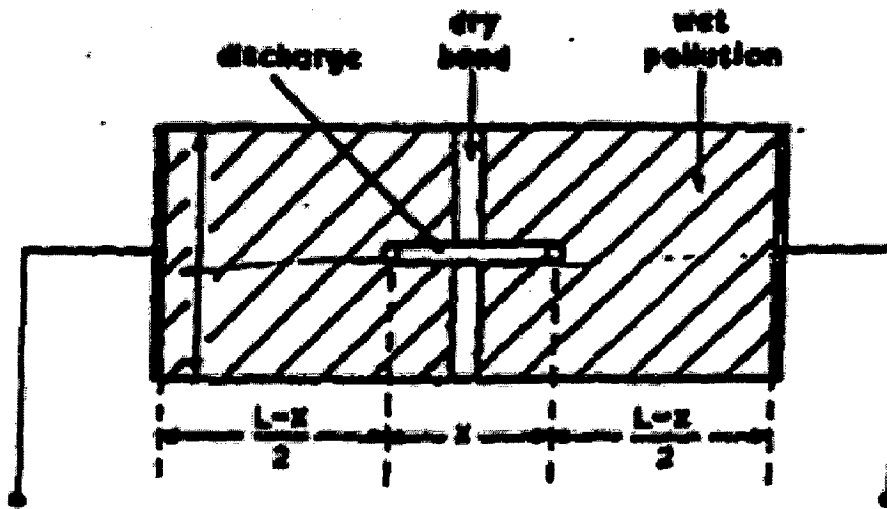


Figure 4.1: Details of Flat Plate Model

For narrow strip, resistance is given as:-

$$R = 1 / (2\pi\sigma s) \{ \pi(L - x) / a + \ln(a / (2\pi r_d)) \}$$

Where,

a = dry band length

σ = surface conductivity

r_d = radius of discharge

Critical voltage for this model is calculated, which is given below:-

$$V_c = N \frac{1}{n+1} r_p \frac{n}{n+1} \{ L + (\frac{a}{2\pi}) \ln(J \frac{a^2}{4\pi i_c}) \} + V_c$$

Where

$$J = \text{current density in amp/cm}^2$$

In the above equation use the surface conductivity i.e. the conductivity at the time of flashover which is affected by high temperature. Therefore the flashover voltage values from these equations give higher values when compared with experimental values. This value may be divided by a suggested factor of about "1.8" to take into account the variation in conductivity due to temperature.

[D] Model of P Claverie

This model deals with the phenomenon of flashover mechanism. Discharge development is studied using a flat plate of glazed porcelain and movement of arc is studied by using a high speed camera. The circuit resistance of pollution in series with the arc is considered with arc ignition conditions. Formula for arc voltage is derived, together with voltage required for re-ignition. Condition e.g. maximum arc length and resistance of pollution layer at maximum arc length is derived. Formula for critical arc length and flashover voltage are derived and applied to practical insulator. In this model criterion for reigniting of arc is developed. For calculating this some assumptions are made here:-

- Arc propagation speed prior to critical conditions so low as to justify the quasi-stationary analysis.
- Single arc flash is assumed.
- Uniform resistivity is assumed.
- It is assumed that the arc propagation is due to the thermal phenomenon, i.e. the arc grows due to heat energy, as it dries the layer in front of the root.

After performing several experiments, arc re-ignition voltage was found to be empirically given by the relation:

$$V > 940 \frac{x}{(I^2)}$$

According to the above formula, if an arc will occur, then to stabilize the glow, the above condition must be satisfied..

Flashover voltage is calculated by following formula:

$$V_c = 47.6 r_p^{\frac{1}{3}} L$$

[E] Model of P.S. Ghosh and S. Chatterjee

A mathematical model to predict the flashover voltage of polluted insulator under AC is presented. This model takes into consideration the appropriate arc constants for different chemical nature of pollutants. The critical values of flashover voltage and current are derived .

$$V_c = L k^{\frac{1}{(n+1)}} N^{\frac{1}{(n+1)}} r_p^{\frac{n}{(n+1)}}$$

$$i_c = \left[\frac{k N}{r_p} \right]^{\frac{1}{n+1}}$$

In this model the value of N=450 and n= 0.49 for NaCl electrolyte are used.

4.3 Cylindrical Models

[A] Model of L.L. Alston & S.Zoledziowski

This model consist of a cylindrical insulator of length “L”, with electrodes on flat ends, as shown in Figure 4.2 below

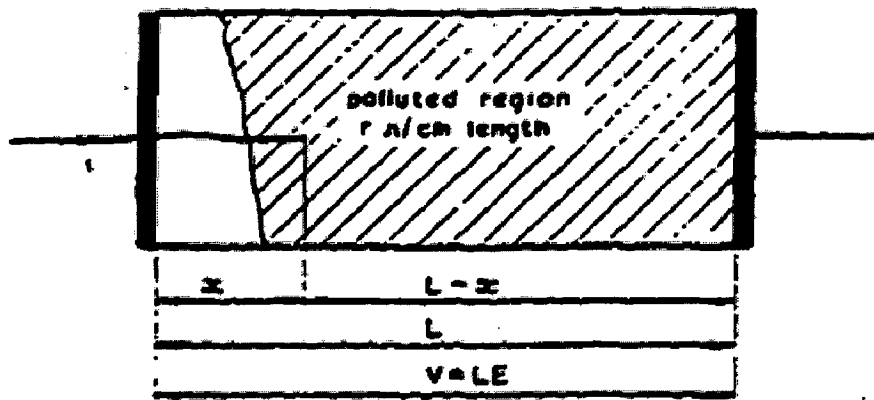


Figure 4.2: Configuration of the model

The voltage required to maintain the discharge on polluted insulators may increase with an increase in discharge length, and if this voltage exceeds the supply voltage, the discharge extinguishes without causing a flashover. Based on this mechanism, criteria, which define flashover conditions, have been developed. A simple geometry of insulator with constant surface resistance per unit length is considered. Flashover criteria in terms of formulae relating to applied voltage; critical stress, discharge length and resistance have been developed. Flashover is considered impossible if the applied voltage and the initial arc length are less than the critical values defined in this model.

In this there was certain assumption made, which are given below:

- Discharge current is constant along the length of the discharge, there is no contact between the discharge and pollution except that at discharge tip.
- The dry band does not conduct the current.
- The electrode voltage drop is neglected.
- Resistance per unit length is constant.
- The electric field is uniform for most part of length.
- Single arc is assumed.

The discharge voltage calculated in this model is given as:-

$$V_{cx} = (n + 1)(N x)^{\frac{1}{n+1}} \left\{ (L - x) \frac{r p}{n} \right\}^{\frac{n}{n+1}}$$

In Figure 4.3 below, plot between “x” and V_{cx} is given:- x_s

As from Figure 4.3 we can see that V_{cx} has maximum value, called critical value V_c . For an applied voltage V_s , the arc can elongate up to an initial length of x_s , as for length greater than x_s , the voltage required to maintain the arc is more than the supply voltage.

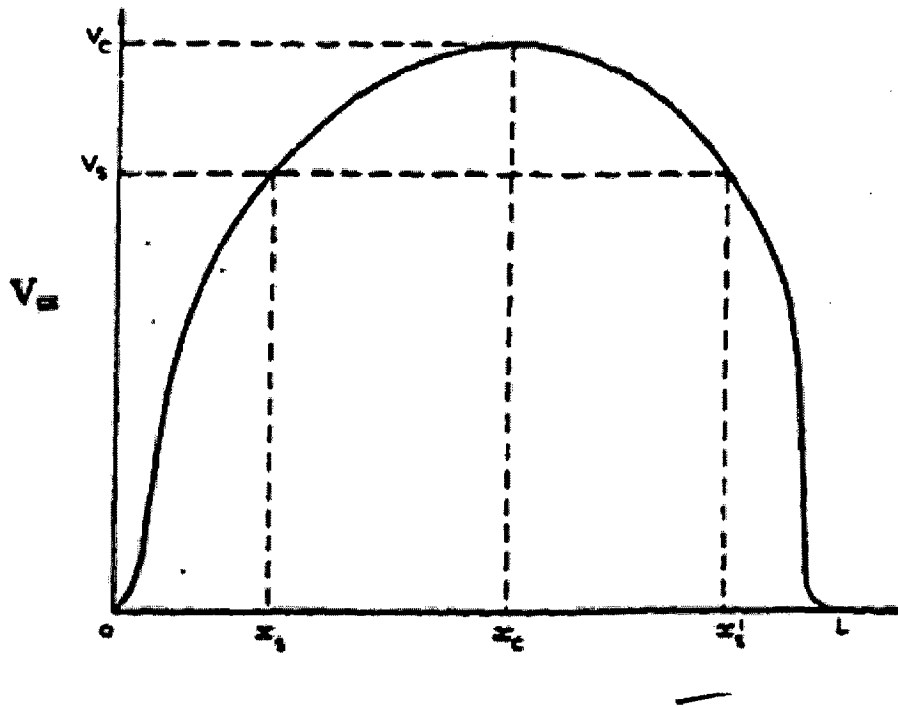


Figure 4.3: Dependence of V_{cx} on arc length

4.4 Summary

Various theories have been proposed to explain the phenomenon of flashover in polluted insulators. This chapter attempts to discuss some of the diverse theories that have been forwarded. It is seen that despite considerable research work, the processes involved in flashover

are still not fully understood.. The process of flashover depends on factors such as type and nature of pollutant, non-uniform wetting process, conductivity of wet layer, orientation, shape and profile of insulator, wind, location, etc. The researcher may experience a formidable task in developing a suitable theory or model, which can explain the phenomenon satisfactorily in terms of all the factors. Since it is impossible to account all the factors involved, therefore the researchers has to make some assumptions in developing these models. It is therefore not surprising to come across different theories explaining flashover mechanism.

In view of this difficulty, researchers need to explore other types of models that can provide reasonable accuracy in predictions. *Artificial Neural Networks(ANN)* based models appear to be promising in this respect and, are therefore the focus of the present dissertation work. The next chapter provides an overview of *ANN* models. The present dissertation attempts to develop a suitable *ANN* model of high accuracy for predicting flashover voltages of polluted insulators.

ARTIFICIAL NEURAL NETWORK (ANN)

- AN OVERVIEW

5.1 Introduction

The neural network was inspired from its inception by the recognition that the human brain computes differently than that of a conventional digital computer. The brain acts as a highly complex, nonlinear, and parallel computer. A neural network is a massively parallel-distributed processor made up of simple processing units, known as neurons, which has a propensity for storing, and making easily available, experiential knowledge. It resembles the brain in two respects:

1. Knowledge is acquired by the network from its environment through learning processes.
2. Inter-neuron connection strengths, known as synaptic weights, are used to store the acquired knowledge.

The procedure used to set the connection strengths is called learning, the function of which is to modify the synaptic weights of the network in an orderly fashion to attain a desired design objective. A neural network derives its computing power through its massively parallel distributed structure and its ability to learn and therefore generalize. Generalization refers to the neural network producing reasonable outputs for inputs not encountered during training (learning). These two information-processing capabilities make it possible for neural networks to solve complex problems. In practice, neural networks often cannot provide adequate solutions by working individually. Rather, they need to be integrated into a consistent system engineering approach. Specifically, a complex problem of interest is decomposed into a number of relatively simple tasks, and neural networks are assigned to a subset of the tasks that match their inherent capabilities. In

this work, the neural networks method is integrated into a system approach for power system voltage security analysis.

5.2 Properties of Artificial Neural Networks [20]

The use of neural networks offers the following useful properties and capabilities:

1. Nonlinearity.

A neural network, made up of an interconnection of nonlinear neurons, is itself nonlinear. Moreover, the nonlinearity is of a special kind in the sense that it is distributed throughout the network. Most real systems, including power systems are nonlinear, so this property is very desirable for its applications in power systems.

2. Input-Output Mapping.

A popular paradigm of learning called learning with a teacher or supervised learning involves modification of the synaptic weights of a neural network by applying a set of labeled training samples or task examples. Each example consists of a unique input signal and a corresponding desired response. The network learns from the examples by constructing an input-output mapping for the problem. In power system voltage security analysis, the traditional approaches which are widely used can be used to generate those training samples.

3. Adaptivity

Neural networks have a built-in capability to adapt their synaptic weights to changes in the surrounding environment. In particular, a neural network trained to operate in a specific environment can be easily retrained to deal with minor changes in the operating environmental conditions. Moreover, when it is operating in a non-stationary environment, a neural network can be designed to change its synaptic weights in real time.

4. Fault tolerance

A neural network has the potential to be inherently fault tolerant in the sense that its performance degrades gracefully under missing or erroneous data. The reason is that the information is

distributed in the network, the errors must be extensive before catastrophic failure occurs. These are the properties that are most desirable for solving the problems at hand. See [24] for a discussion of other useful properties.

5.3 The Model of a Neuron [20]

A neuron is an information-processing unit that is fundamental to the operation of a neural network. Figure 5.1 shows a model of neuron. There are three basic elements:

1. A set of synapses or connecting links, each of which is characterized by a weight or strength of its own.

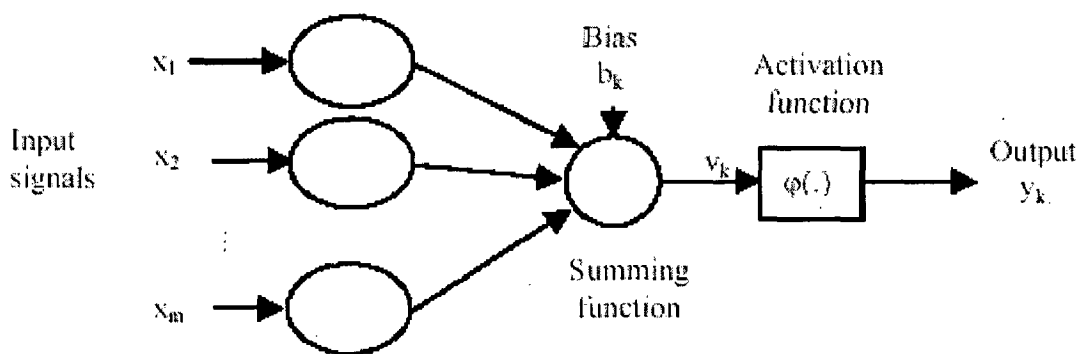


Figure 5.1 Model of a neuron

2. An adder for summing the input signals, weighted by the respective synapses of the neuron; the operations by the adder constitute a linear combiner.
3. An activation function for limiting the amplitude of the output of a neuron. Typically, it constrains the amplitude of the output signals to lie within the intervals $[0, 1]$ or $[-1, 1]$.

The neuron in Figure 5.1 also includes an externally applied bias, denoted by b_k . The bias b_k has the effect of increasing, or lowering, the net input of the activation function, depending on whether it is positive, or negative. The activation function, denoted by $\phi(v)$, defines the output of a neuron in terms of the induced local field v . There are basically three different kinds of activation functions:

1. Threshold function. $\varphi(v) = \begin{cases} 1 & \text{if } v \geq 0 \\ 0 & \text{if } v < 0 \end{cases}$

2. Piecewise-linear function. $\varphi(v) = \begin{cases} 1 & \text{if } v \geq \frac{1}{2} \\ v & \text{if } \frac{1}{2} > v > -\frac{1}{2} \\ 0 & \text{if } v \leq -\frac{1}{2} \end{cases}$

3. $\varphi(v) = \frac{1}{1 + \exp(-av)}$ Sigmoidal functions, including the logistic function: and

The hyperbolic $\varphi(v) = \tanh(v) = \frac{1 - \exp(-v)}{1 + \exp(v)}$ tangent function: as shown in

Figure 5.2 (a) and (b).

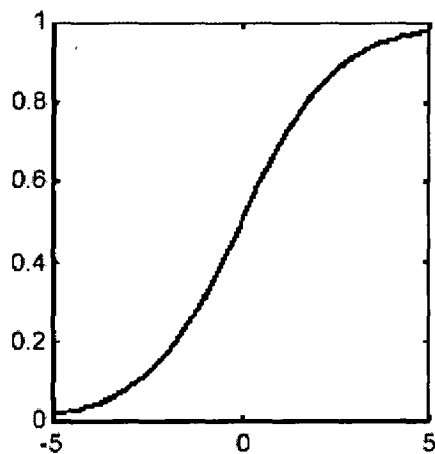


Figure 5.2(a) Logistic function

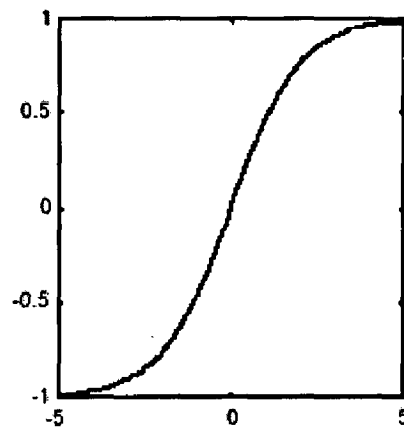


Figure 5.2(b) Hyperbolic tangent function

5.4 Learning Processes [20]

Learning is a process by which the free parameters of a neural network are adapted through stimulation by the environment in which the network is embedded. The type of learning is determined by the manner in which the parameter changes take place. The property that is of primary significance for a neural network is the ability of the network to learn from its environment, and to improve its performance through learning. A neural network learns about its environment through an interactive process of adjustments applied to its synaptic weights and bias levels. Ideally, the network becomes more knowledgeable about the environment after each

iteration of the learning process. There are five basic learning rules: error-correction learning, memory-based learning, *Hebbian* learning, competitive learning, and *Boltzmann* learning.

5.4.1 Error-Correction Learning

Error-correction learning is based on optimum filtering and is used in feed forward networks, which are employed by this study. To illustrate the learning rule, consider the simple case of a neuron k constituting the only computational node in the output layer of a feed forward neural network, as depicted in Figure 5.3.

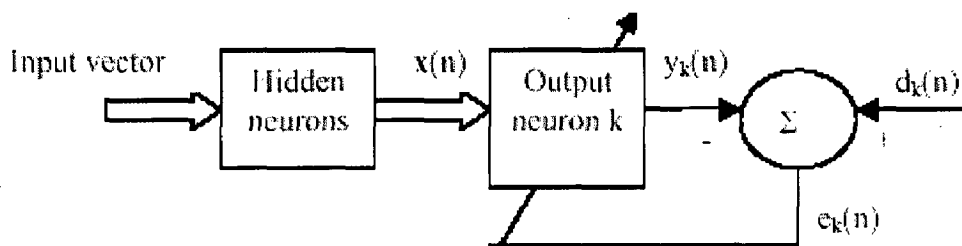


Figure 5.3 Feedback in Network

The output signal $y_k(n)$, representing the only output of the neural network, is compared to a desired response or target output, $d_k(n)$. Consequently, an error signal, $e_k(n)$, is produced, where $e_k(n) = d_k(n) - y_k(n)$. The error signal $e_k(n)$ actuates a control mechanism, the purpose of which is to apply a sequence of corrective adjustments to the synaptic weights of neuron k . The corrective adjustments are designed to make the output signal $y_k(n)$ approach the desired response $d_k(n)$ in a step-by-step manner. This objective is achieved by minimizing a cost function or index of performance, $\epsilon(n) = 0.5 e_k^2(n)$. That is, $\epsilon(n)$ is the instantaneous value of the error energy. The step-by-step adjustments to the synaptic weights of neuron k are continued until the system reaches steady state (i.e., the synaptic weights are essentially stabilized).

Minimization of the cost function $\epsilon(n)$ leads to a learning rule commonly referred to as the delta rule or *Widrow-Hoff* rule:

$$\Delta w_{kj}(n) = \eta e_k(n) x_j(n)$$

where $w_{kj}(n)$ is the weight of neuron k excited by $x_j(n)$ of the signal vector $x(n)$ at time step n . η is a positive constant that determines the rate of learning.

5.4.2 Memory-Based Learning

Memory-based learning operates by memorizing the training data explicitly. All (or most) of the past experiences are explicitly stored in a large memory of correctly classified input-output examples as

$\{X_i, d_i\}_{i=0}^N$ where X_i denotes an input vector and d_i denotes the corresponding desired response.

All memory-based learning algorithms involve two essential ingredients:

- (1) A criterion for defining the local neighborhood of the test vector x_{test} , and,
- (2) A learning rule applied to the training examples in the local neighborhood of x_{test} .

In a simple, yet effective type of memory-based learning, known as the nearest neighbor rule, the local neighborhood is defined as the training example that lies in the immediate neighborhood of the test vector x_{test} . In particular, the vector $X'N \in \{x_1, x_2, \dots, x_N\}$. x is said to be the nearest neighbor of x_{test} if $\min_i d(x_i, x_{test}) = d(X'N, x_{test})$ where $d(x_i, x_{test})$ is the Euclidean distance between the vectors x_i and x_{test} . The class associated with the minimum distance, that is, vector $x'N$, is reported as the classification of x_{test} .

5.4.3 Hebbian Learning

Hebb's postulate learning is the oldest and most famous of all learning rules; it is named in honor of the neuropsychologist Hebb. It has two parts :

- (a) If two neurons on either side of a synapse (connection) are activated simultaneously, then the strength of that synapse is increased.
- (b) If two neurons on either side of a synapse are activated asynchronously, then that synapse is weakened or eliminated.

One form of *Hebbian* learning is using covariance hypothesis:

$$\Delta w_{kj} = \eta(x_i - x)(y_k - y)$$

where η is the learning-rate parameter. x and y are the time-averaged values of the pre-synaptic signal, x_i , and postsynaptic, y_k , respectively. One can see from (2.2) that synaptic weight w_{ij} is enhanced if there are sufficient levels of pre-synaptic and postsynaptic activities. Synaptic weight w_{ij} is depressed if there is either a pre-synaptic activation in the absence of sufficient postsynaptic activation or a postsynaptic activation in the absence of sufficient pre-synaptic activation. There is strong physiological evidence for *Hebbian* learning in the area of the brain called the hippocampus. This physiological evidence provides *Hebbian* learning with significant justification.

5.4.4 Competitive Learning

Competitive learning is also inspired by neurobiological considerations. The output neurons of a neural network compete among themselves to become active (fired). Whereas in a neural network based on *Hebbian* learning several output neurons may be active simultaneously, in competitive learning only a single output neuron is active at any one time. It is this feature that makes competitive learning highly suited to discover statistically salient features that may be used to classify a set of input patterns. The individual neurons of the network learn to specialize on ensembles of similar patterns; in doing so they become feature detectors for different classes of input patterns. The standard competitive learning rule defines change of weight by

$$\Delta w_{kj} = \begin{cases} \eta(x_j - w_{kj}) & \text{if neuron } k \text{ wins} \\ 0 & \text{else} \end{cases} \quad (2.3)$$

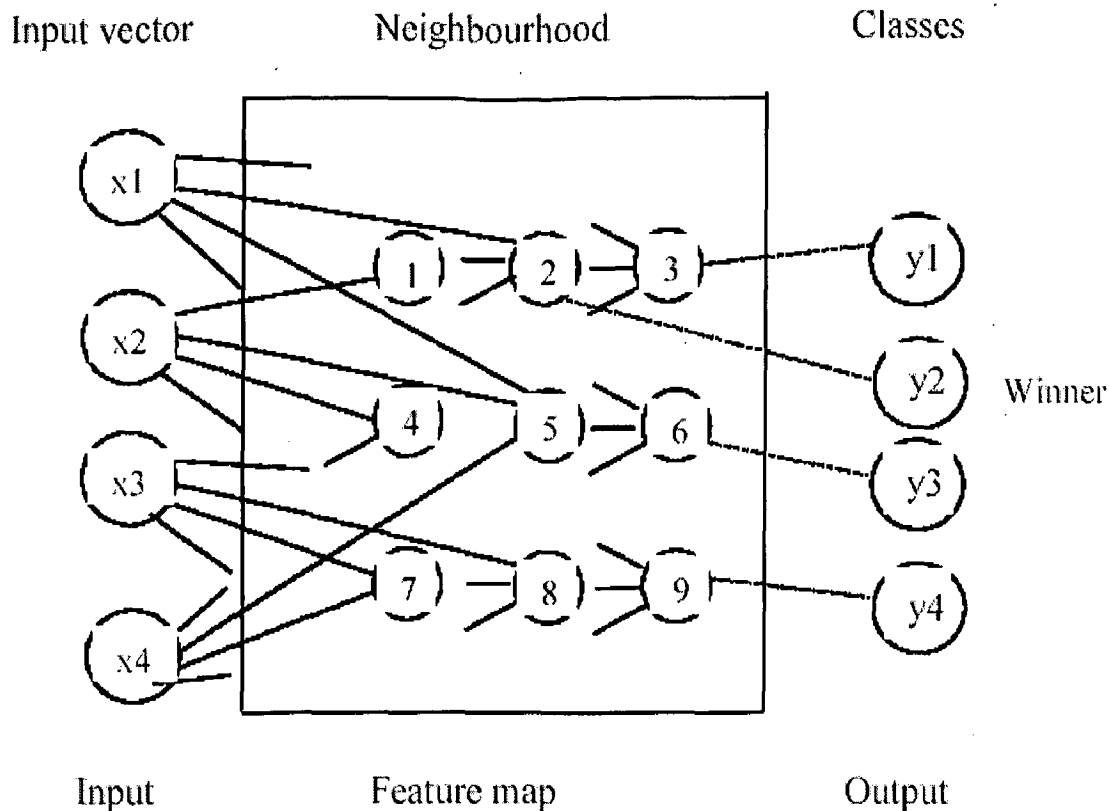


Figure 5.4 Kohonen networks

This rule has the overall effect of moving the synaptic weight vector w_k of winning neuron k toward the input pattern x . This kind of learning is used in *Kohonen maps*.

5.4.5 Boltzmann Learning

The *Boltzmann* learning rule, named in honor of Ludwig Boltzmann, is a stochastic learning algorithm derived from ideas rooted in statistical mechanics. A neural network designed on the basis of the *Boltzmann* learning rule is called a *Boltzmann* machine. The machine is characterized by an energy function:

$$E = -\frac{1}{2} \sum_j \sum_k w_{kj} x_k x_j \quad j \neq k$$

The machine operates by choosing a neuron at random at some step of the learning process, then flipping the state of neuron from state x_k to $-x_k$ at some temperature T with probability

$$P = \frac{1}{1 + \exp(-\Delta E_k / T)},$$

where E_k is the energy change resulting from such a flip.

If this rule is applied repeatedly, the machine will reach thermal equilibrium. The learning rule is defined by

$$\Delta w_{kj} = \eta(\rho_{kj}^+ - \rho_{kj}^-), \quad j \neq k$$

where ρ_{kj}^+ and ρ_{kj}^- denote the correlation between the states of neurons k and j with the network in its clamped condition (visible neurons are all fixed into specific states determined by the environment) and free-running condition, respectively.

5.5 Kohonen Self-Organizing Networks

Kohonen self-organizing networks are competitive-based network paradigm for data clustering. Networks of this type impose a neighborhood constraint on the output units, such that a certain topological property in the input data is reflected in the output units' weights. Figure 5.4 shows a *Kohonen* network. Based on competitive learning, *Kohonen* networks use a similarity measure. The winning unit is considered to be the one with the largest activation. For *Kohonen* feature maps, however, one updates not only the winning unit's weights but also all of the weights in a neighborhood around the winning units. The neighborhood's size generally decreases slowly with each iteration. A sequential description of how to train a *Kohonen* self organizing network is as follows:

- (1) Select the winning output unit as the one with the largest similarity measure between all weight vectors w_i and the input vector x . If the Euclidean distance is chosen as the dissimilarity measure, then the winning unit c satisfies the following equation:

$$\|x - \mathbf{w}_c\| = \min_i \|x - \mathbf{w}_i\|$$

(2) Let NB_c denote a set of indices corresponding to a neighborhood around winner c . The weights of the winner and its neighboring units are then updated by:

$$\Delta w_i = \eta(\mathbf{x} - \mathbf{w}_i) \quad i \in NB_c$$

Instead of defining the neighborhood of a winning unit, one can also use a neighborhood function $\Omega_c(i)$ around a winning unit c . For instance, the Gaussian function can be used as the neighborhood function:

$$\Omega_c(i) = \exp\left(\frac{-\|p_i - p_c\|^2}{2\sigma^2}\right)$$

where p_i and p_c are the positions of the output units i and c , respectively, and σ reflects the scope of the neighborhood. By using the neighborhood function, the update formula can be rewritten as:

$$\Delta w_i = \eta \Omega_c(i)(\mathbf{x} - \mathbf{w}_i)$$

where i is the index for all output units. To achieve better convergence, the learning rate and the size of neighborhood should be decreased gradually with each iteration.

5.6 Multilayer Perception [20]

5.6.1 Introduction

Multilayer perception network consists of a set of sensory units (source nodes) that constitute the input layer, one or more hidden layers of computation nodes, and an output layer of computation nodes. The input signal propagates through the network in a forward direction, on a layer-by-layer basis. Multilayer perceptions have been applied successfully to solve a number of diverse and

difficult problems by training them in a supervised manner with a highly popular algorithm known as the back-propagation algorithm. This algorithm is based on the error-correction learning rule. Error back-propagation learning consists of two passes through the different layers of the network: a forward pass and a backward pass. In the forward pass, an activity pattern (input vector) is applied to the sensory nodes of the network, and its effect propagates through the network layer by layer. Next, a set of outputs is produced as the actual response of the network. During the forward pass the synaptic weights of the networks are all fixed. During the backward pass, on the other hand, the synaptic weights are all adjusted in accordance with an error-correction rule. Specifically, the actual response of the network is subtracted from a desired response to produce an error signal. This error signal is then propagated backward through the network against the direction of synaptic connections-hence the name “error back-propagation.” The synaptic weights are adjusted to make the actual response of the network move closer to the desired response in a statistical sense.

5.6.2 Error Back-Propagation Algorithm

The back propagation algorithm is defined using delta rule:

$$\Delta w_{\mu}(n) = \eta \delta_j(n) y_i(n)$$

where $y_i(n)$ is the input signal of neuron j from neuron i and $\delta_j(n)$ is the local gradient. If neuron j is an output node, $\delta_j(n)$ equals the product of the derivative $\varphi_j'(v_j(n))$ and the error signal $e_j(n)$, both of which are associated with neuron j , i.e., $\delta_j(n) = e_j(n) \varphi_j'(v_j(n))$. If neuron j is a hidden node, $\delta_j(n) = \varphi_j'(v_j(n)) \sum_k \delta_k(n) w_{kj}$, i.e., $\delta_j(n)$ equals the product of the associative derivative $\varphi_j'(v_j(n))$ and the weighted sum of the δ 's computed for the neurons in the next hidden or output layer that are connected to neuron j . The factor $\varphi_j'(v_j(n))$ depends solely on the activation function associated with hidden neuron j . Figure below shows the signal-flow graph of the error

back-propagation algorithm.

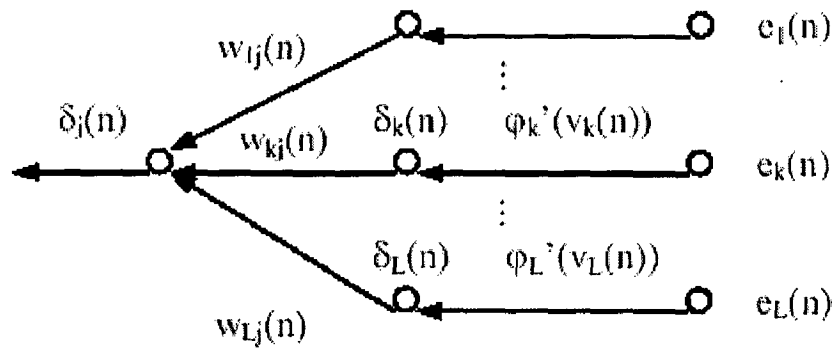


Figure 5.5 Signal-flow graph of the error back-propagation algorithm

5.6.3 Achieving Better Performance

There are many methods that will significantly improve the back-propagation algorithm performance. A few are briefly described here:

- (1) The sequential mode of back-propagation learning is computationally faster than the batch mode. This is especially true when the training data set is large and highly redundant.
 - (2) The use of an example that results in the largest training error or an example that is radically different from all those previously used. This will maximize information content. These two heuristics are motivated by a desire to search more of the weight space.
 - (3) Generally, using an ant symmetric activation function is faster than using nonsymmetrical functions in back-propagation.
 - (4) Normalizing the inputs and target values will keep the back-propagation algorithm away from the limiting value of the sigmoid activation function. Otherwise, the backpropagation algorithm tends to drive the free parameters of the network to infinity, and thereby slow down the learning process by forcing the hidden neurons into saturation.
- The input should be uncorrelated; this can be done using principal component analysis.

The de-correlated input should be scaled so that their covariance's are approximately equal, thereby ensuring that the different synaptic weights in the network learn at approximately the same speed.

(5) A good choice of initialization is important so that too large a value will not drive the network to saturation nor too small a value will cause the network to operate on a very flat area around the origin of the error surface.

(6) A high learning rate will speed up the rate of learning, but the network may become unstable. A simple way of increasing the rate of learning yet avoiding the danger of instability is to modify the delta rule by including a momentum term:

$$\Delta w_{ji}(n) = \alpha \Delta w_{ji}(n-1) + \eta \delta_j(n) y_i(n)$$

where α is usually a positive number called the momentum constant.

5.6.4 Improving Generalization

The essence of back-propagation learning is to encode an input-output mapping into the synaptic weights and thresholds of a multilayer perception. The hope is that the network becomes well trained so that it learns enough about the past to generalize to the future. One problem that occurs during training is called over fitting. The error on the training set is driven to a very small value, but when new data is presented to the network the error is large. The network has memorized the training examples, but it has not learned to generalize to new situations. Use a network that is just large enough to provide an adequate fit will improve network generalization. The larger a network is used the more complex the functions that the network can create. If a small enough network is used, it will not have enough power to over fit the data. The problem is that it is difficult to know beforehand how large a network should be for a specific application.

There are two other methods for improving generalization. The first is modifying the performance function, which is normally chosen to be the sum of squares of the network errors on the training set:

$$F = mse = \frac{1}{N} \sum_{i=1}^N (e_i)^2$$

The modified performance function is then:

$$msereg = \gamma mse + (1 - \gamma)msw$$

where γ is the performance ratio, and $msw = \frac{1}{n} \sum_{j=1}^n w_j^2$.

Using such a performance function will cause the network to have smaller weights and biases, and this will force the network response to be smoother and less likely to over fit. Another method for improving generalization is early stopping. In this technique, the available data is divided into three subsets: training set, validation set and test set. The training set is used for computing the gradient and updating the network weights and biases. The error on the validation set is monitored during the training process to guard against over fit. The validation error will normally decrease during the initial phase of training, as does the training set error. When the network begins to over fit the data, the error on the validation set will typically begin to rise and learning can be stopped. Both methods are used to guard against over fitting.

ARTIFICIAL NEURAL NETWORK (ANN) MODELS FOR FLASH OVER VOLTAGE (FOV) ESTIMATION

6.1 Introduction

In the present chapter an attempt is made to develop suitable *ANN* models for predicting the flashover voltage (FOV) of contaminated insulators. Since different architectures are possible, it is indeed a voluminous task to explore all possible structures. Therefore, the study is restricted to the investigation of a few selected architectures, and the best ANN model from these is selected for subsequent simulation studies.

6.2 The Control Variables

Flash over voltage (FOV) has been experimentally seen to be a function of certain variables. In the study reported by Al-Alawi et al [18], the following variables are found to exert influence:

- (1) Salinity of contaminated salt solution (gm/100 ml)
- (2) Solution current (mA)
- (3) Resistivity of salt solution(ohm-cm)

The output variable is the Flash over voltage (FOV).

Accordingly, The ANN models developed make use of the above three control (input) variables with FOV as the output (controlled) variable.

6.3 Activation Functions

The models make us of activation functions of different functional forms. The following are the activation functions generally available with ANN models:

(a) Linear Transfer Function (**LTF**)

(b) Log- Sigmoid Transfer Function(**LSTF**)

(c) Hyperbolic Tangent Sigmoid Transfer Function.(**HTSTF**)

Various combinations of the above transfer functions may be employed with respect to the hidden layer inputs and the output layer inputs.

6.4 ANN Architectures

The *ANN* models used in the present study have three inputs and a single input. The choice of the number of nodes for a single hidden layer can be varied from three to seven. Therefore, by varying the number of hidden layer nodes, different architectures/configurations have been developed

6.5 ANN Models Developed

Table 6.1 shows the various configurations of models that are considered for the present study:

Table 6.1 ANN Models Configuration

S.No	Model	No. of nodes in input layer	No. of nodes in hidden layer	No. of nodes in output layer	Activation function (Input-hidden layer)	Activation Function (Hidden-output layer)
1.	A	3	5	1	LSTF	LTF
2.	B	3	5	1	LSTF	LSTF
3.	C	3	5	1	LSTF	HTSTF
4.	D	3	5	1	LTF	LTF
5.	E	3	5	1	HTSTF	LSTF
6.	F	3	5	1	HTSTF	LTF
7.	G	3	5	1	HTSTF	HTSTF
8.	H	3	7	1	LSTF	LTF
9.	I	3	7	1	LTF	LTF
10	J	3	3	1	LSTF	LTF

6.6 Software Used

MATLAB version 7.3.0(R2006b) software was used for the purpose of developing the ANN models as described in Table 6.1. The MATLAB Tool Box function was used. Training data for the models was obtained from the experimental data quoted in reference [18]. Due to unavailability of a large number of data sets, the ANN models were trained with limited observational points. Nevertheless, the results show good agreement with the actual data outputs and this validates the application of ANN methodology for prediction of FOV in polluted insulators.

6.7 Results and Discussions

6.7.1 Model Architecture/Configuration and Training

6.7.1.1 Model A

Figure 6.2 shows the structure of Model A as depicted in MATLAB Toolbox:

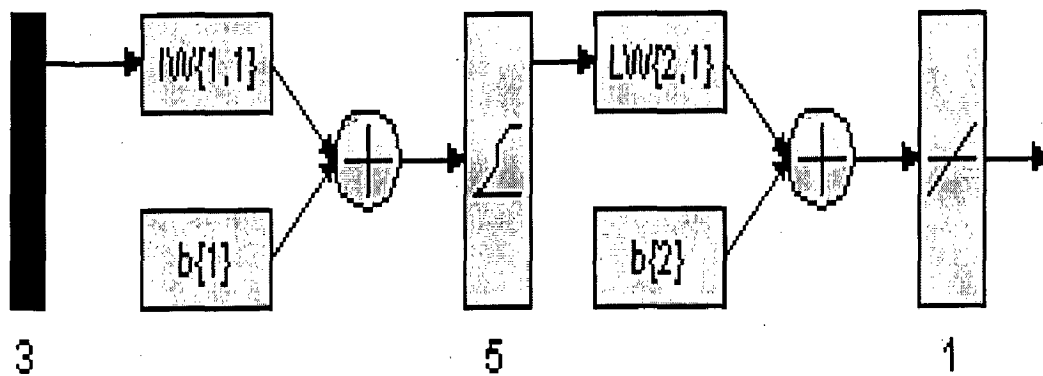


Figure 6.2: Layout of Model A

Training Curve for Model A is shown in Figure 6.3

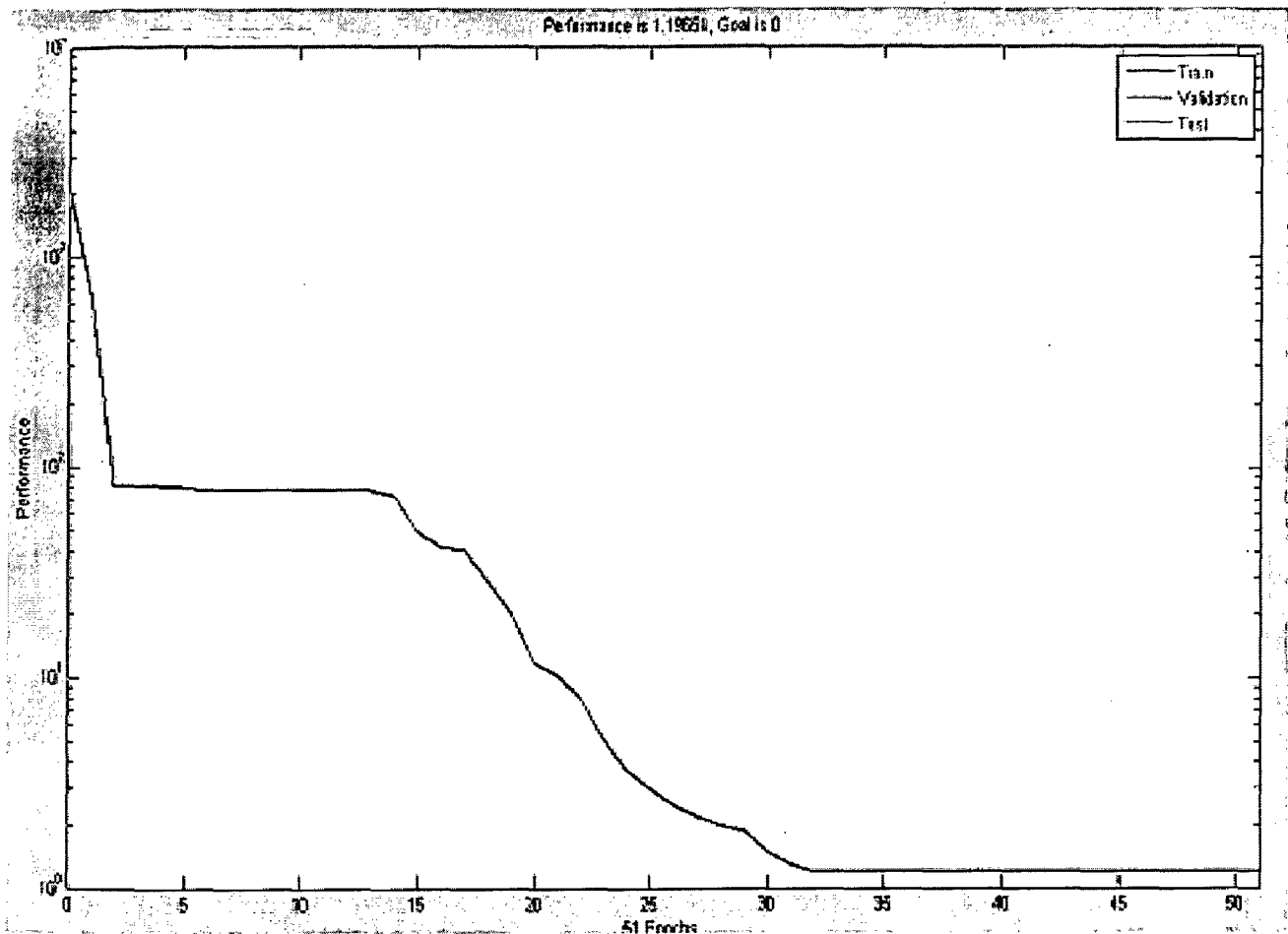


Figure 6.3: Training Curve for Model A

6.7.1.2 Model B

Figure 6.4 shows the structure of Model B as depicted in MATLAB Toolbox:

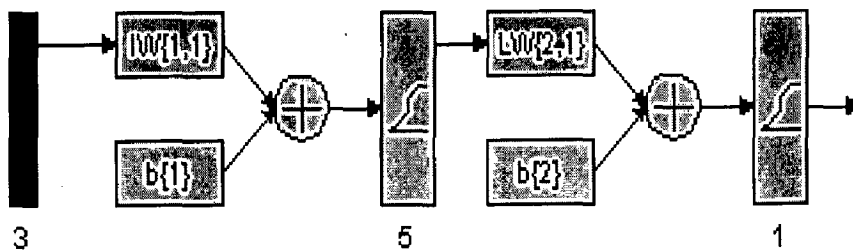


Figure 6.4: Layout of Model B

Training Curve for Model B is shown in Figure 6.5

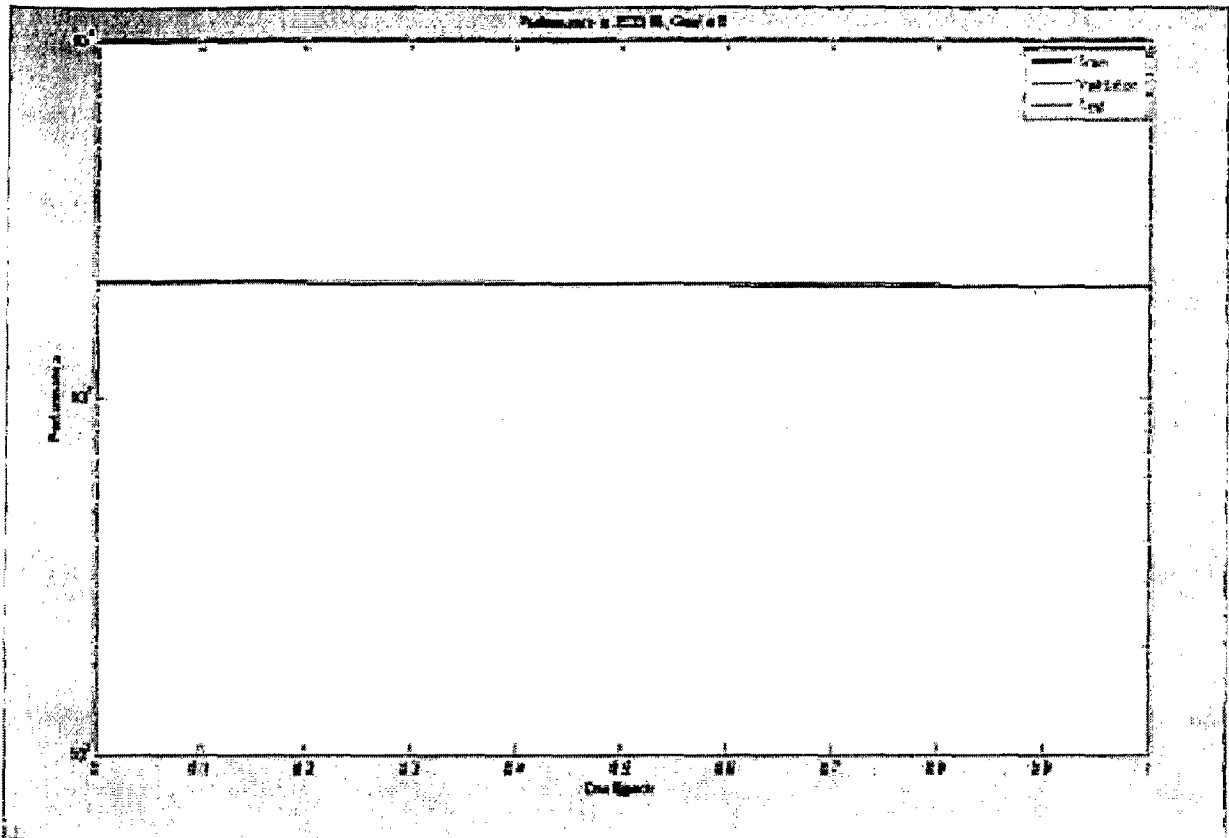


Figure 6.5 Training Curve for Model B

6.7.1.3 Model C

Figure 6.6 shows the structure of Model C as depicted in MATLAB Toolbox:

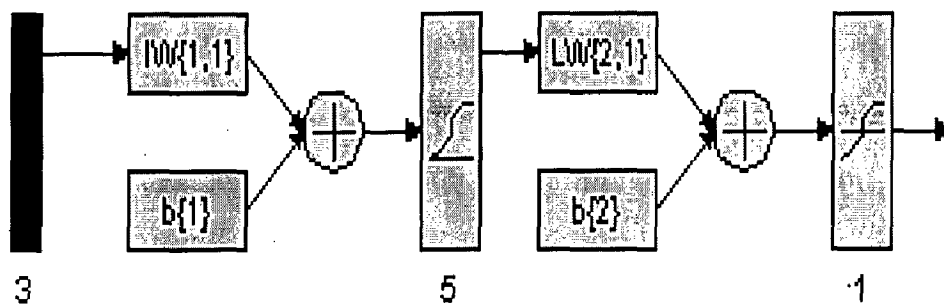


Figure 6.6: Layout of Model C

Training Curve for Model C is shown in Figure 6.7

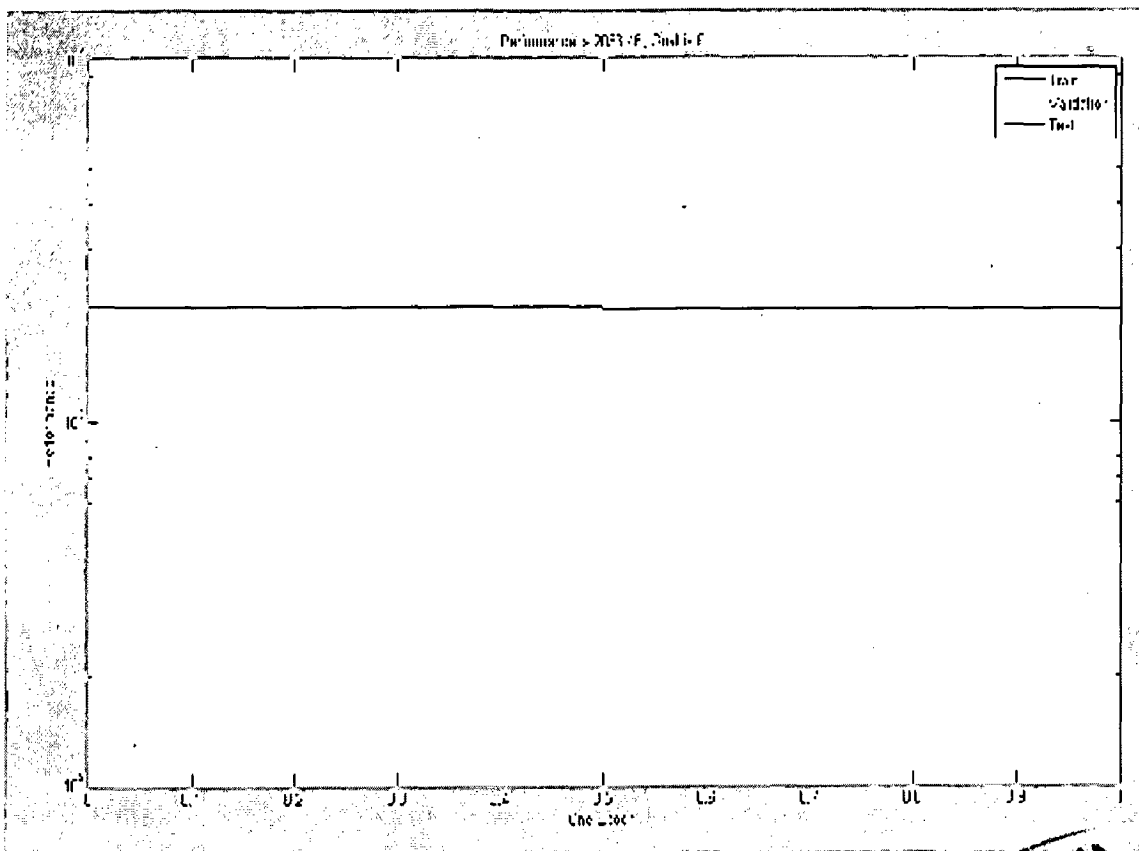
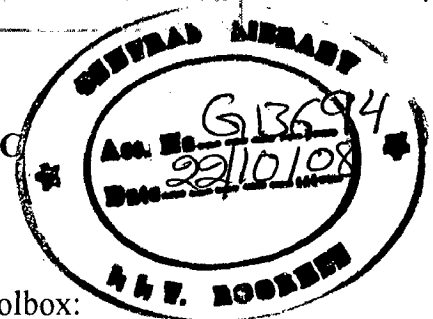


Figure 6.7 Training Curve for Model C



6.7.1.4 Model D

Figure 6.8 shows the structure of Model D as depicted in MATLAB Toolbox:

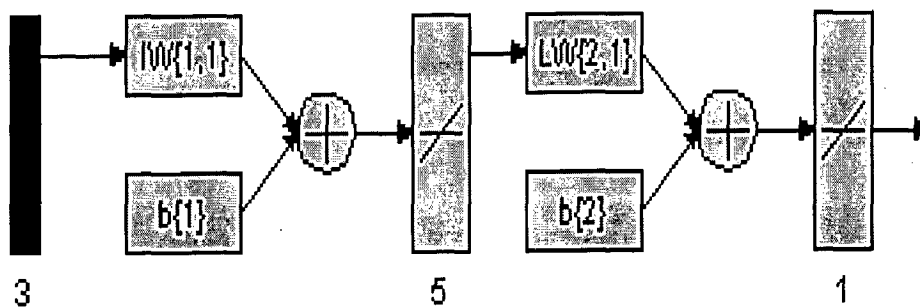


Figure 6.8: Layout of Model D

Training Curve for Model D is shown in Figure 6.9

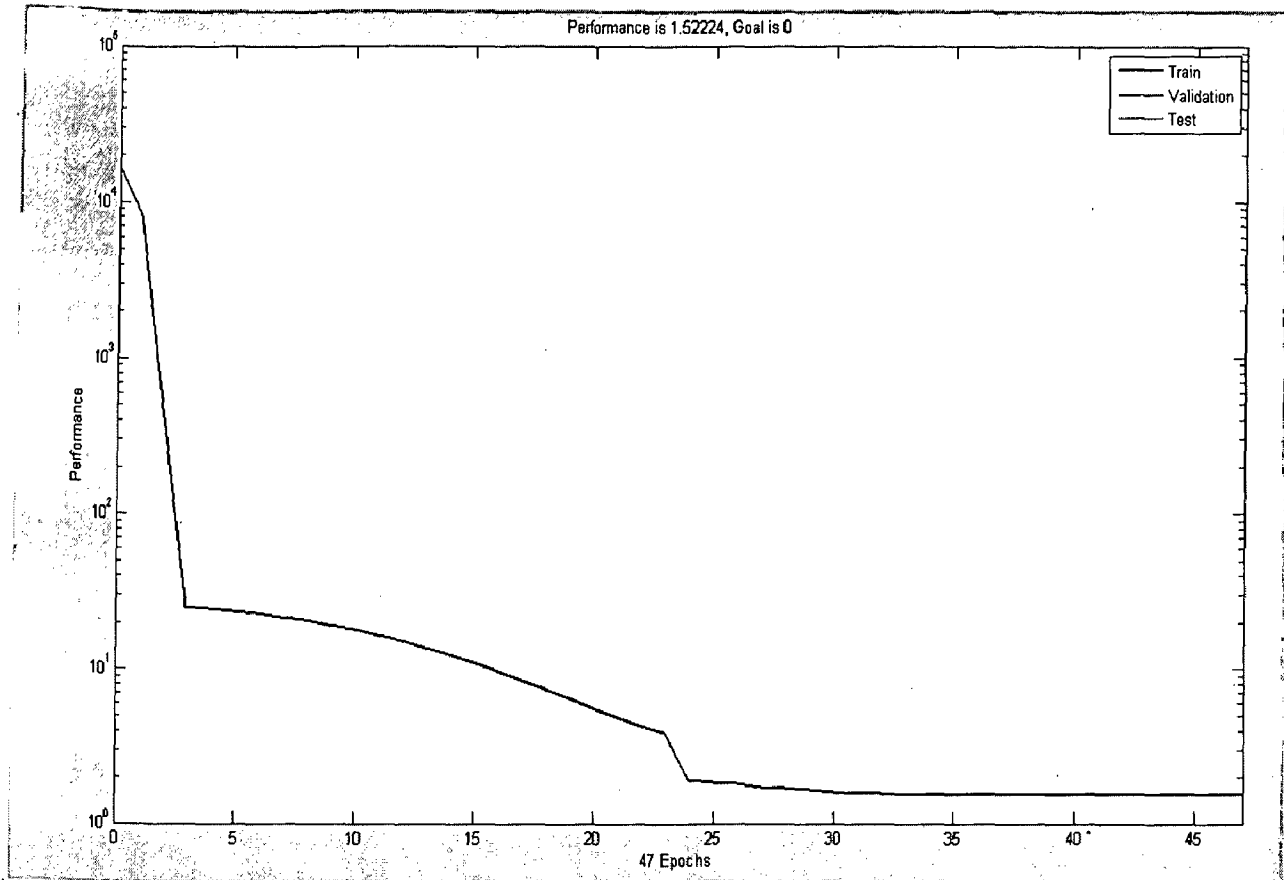


Figure 6.9 Training Curve for Model D

6.7.1.5. Model E

Figure 6.10 shows the structure of Model E as depicted in MATLAB Toolbox:

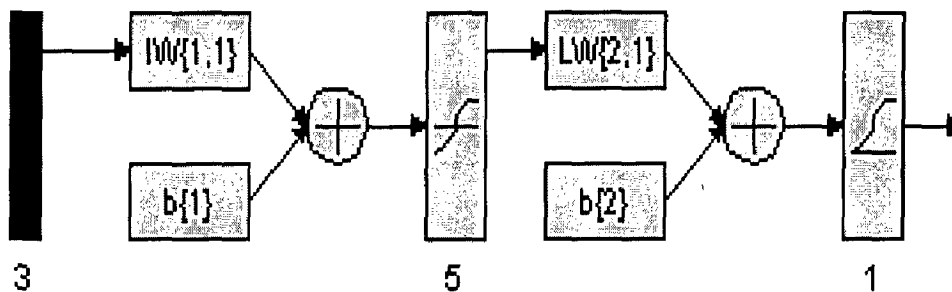


Figure 6.10: Layout of Model E

Training Curve for Model D is shown in Figure 6.11

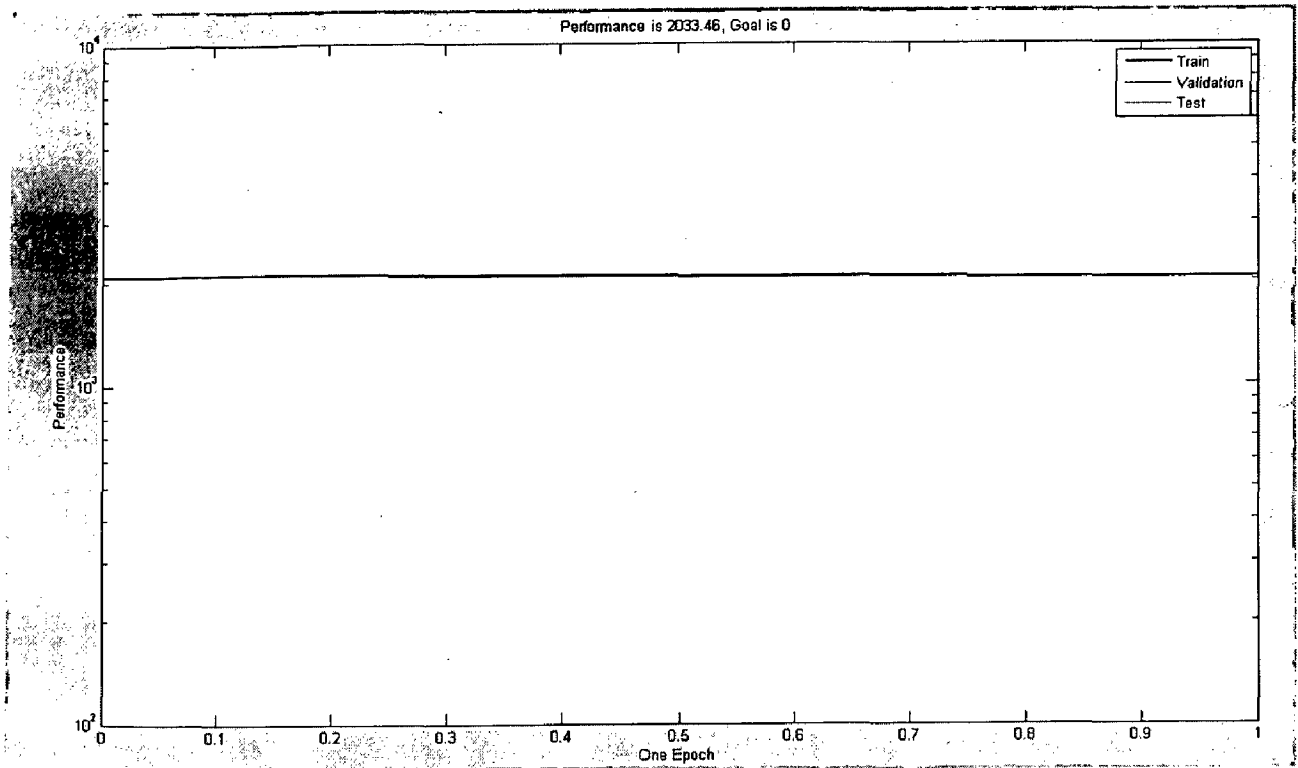


Figure 6.11 Training Curve for Model E

6.7.1.6 Model F

Figure 6.12 shows the structure of Model F as depicted in MATLAB Toolbox:

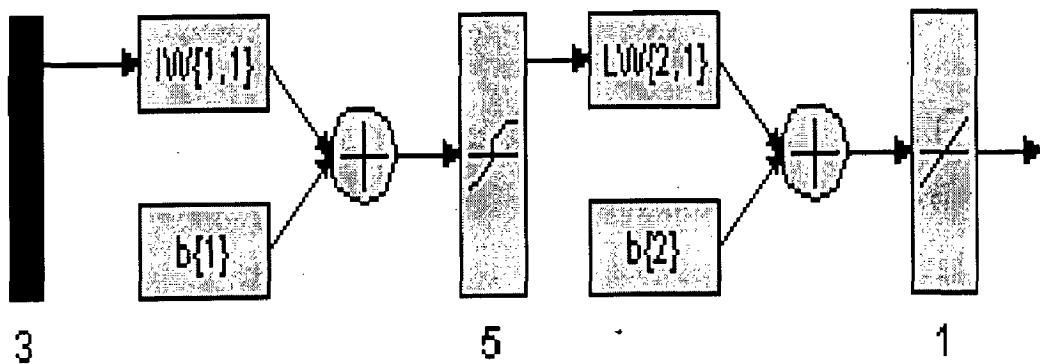


Figure 6.12: Layout of Model F

Training Curve for Model F is shown in Figure 6.13

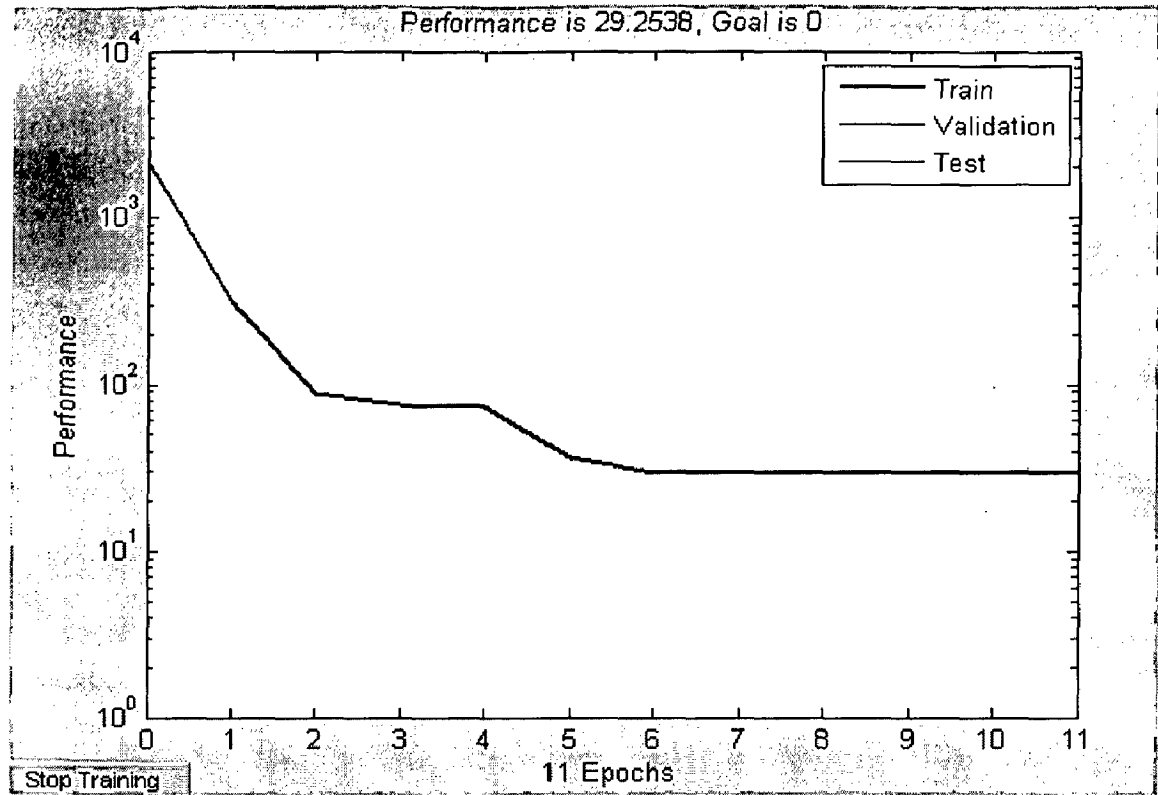


Figure 6.13 Training Curve for Model F

6.7.1.7 Model G

Figure 6.14 shows the structure of Model G as depicted in MATLAB Toolbox:

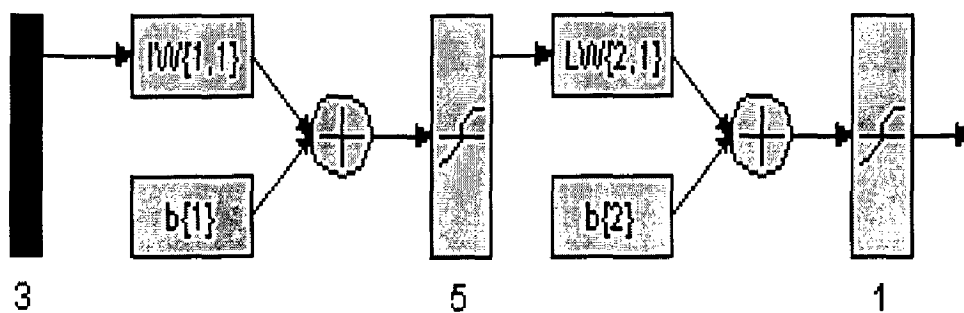


Figure 6.14: Layout of Model G

Training Curve for Model G is shown in Figure 6.15

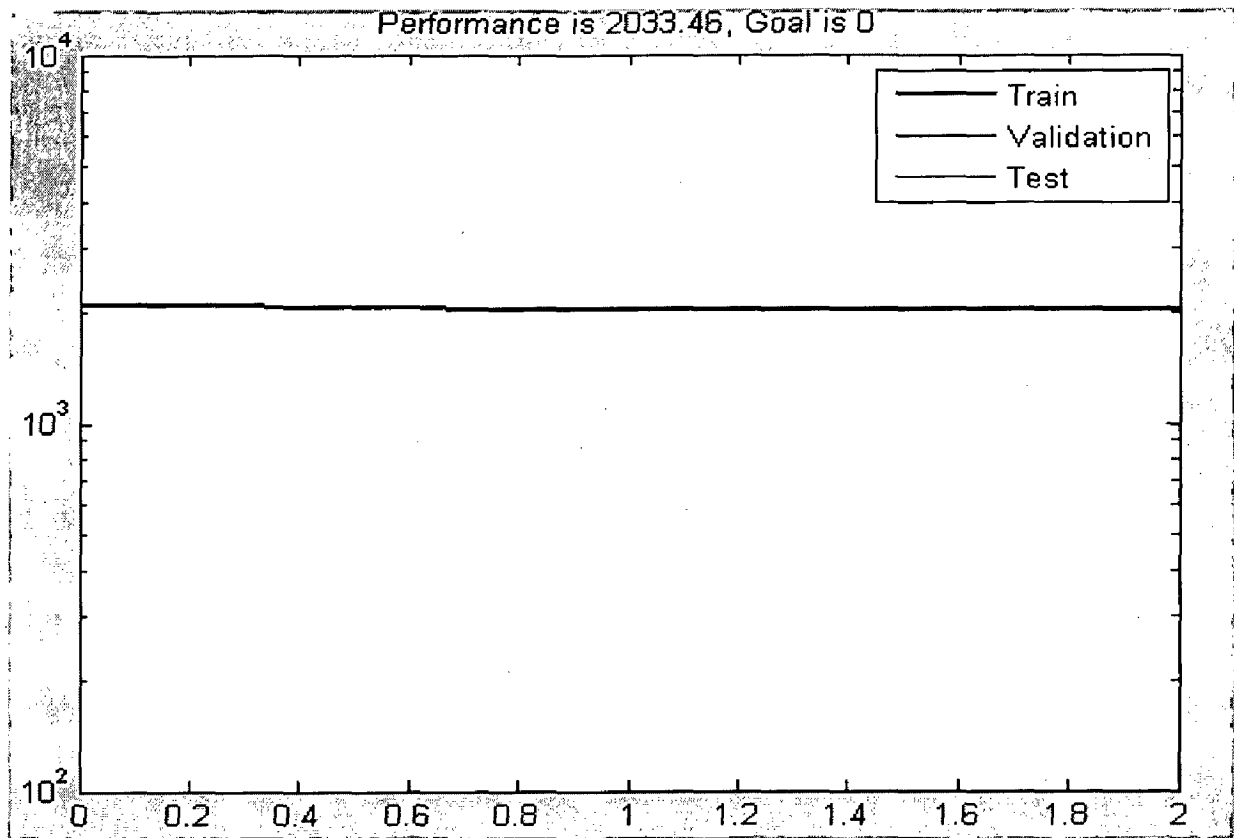


Figure 6.15 Training Curve for Model G

6.7.1.8 Model H

Figure 6.16 shows the structure of Model H as depicted in MATLAB Toolbox:

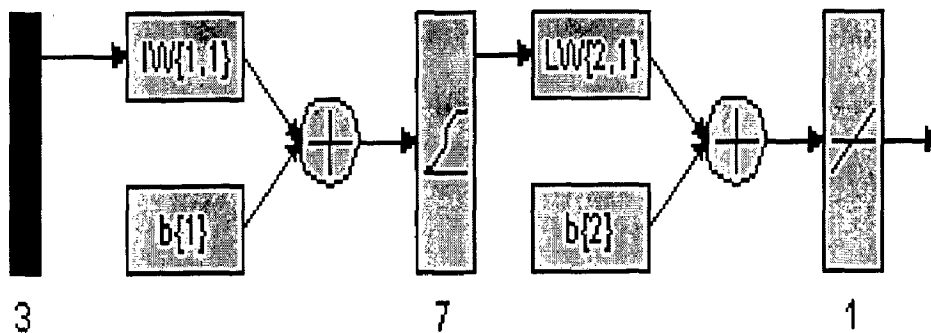


Figure 6.16: Layout of Model H

Training Curve for Model H is shown in Figure 6.17

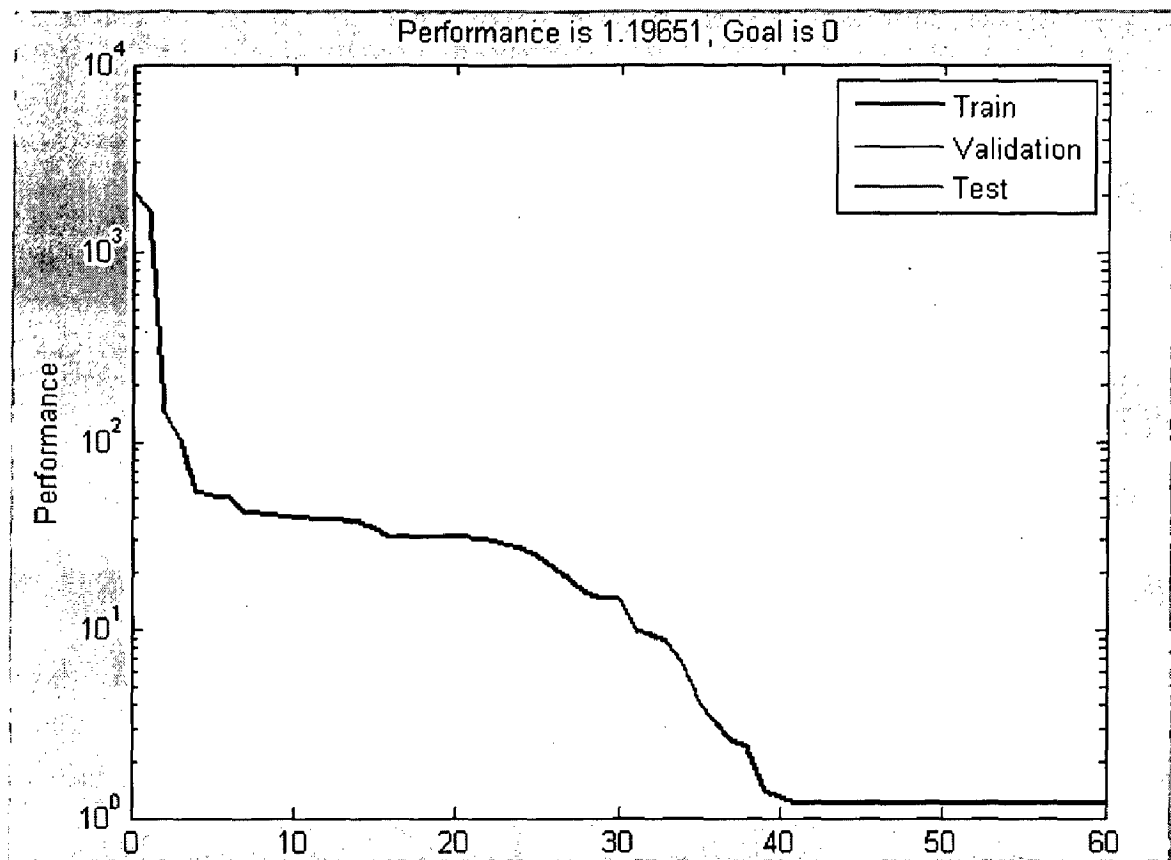


Figure 6.17 Training Curve for Model H

6.7.1.9 Model I

Figure 6.18 shows the structure of Model H as depicted in MATLAB Toolbox:

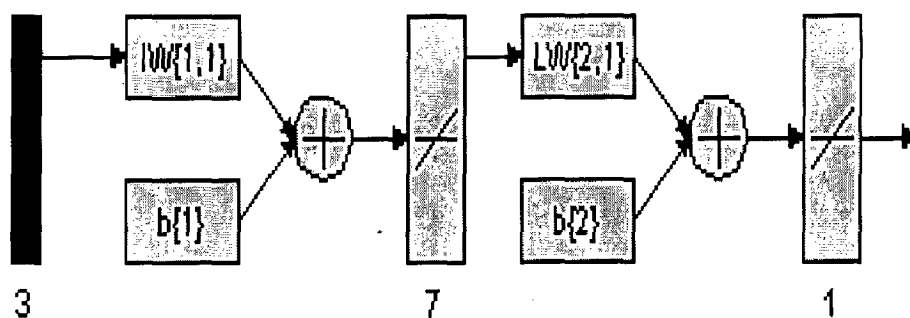


Figure 6.18: Layout of Model I

Training Curve for Model I is shown in Figure 6.19

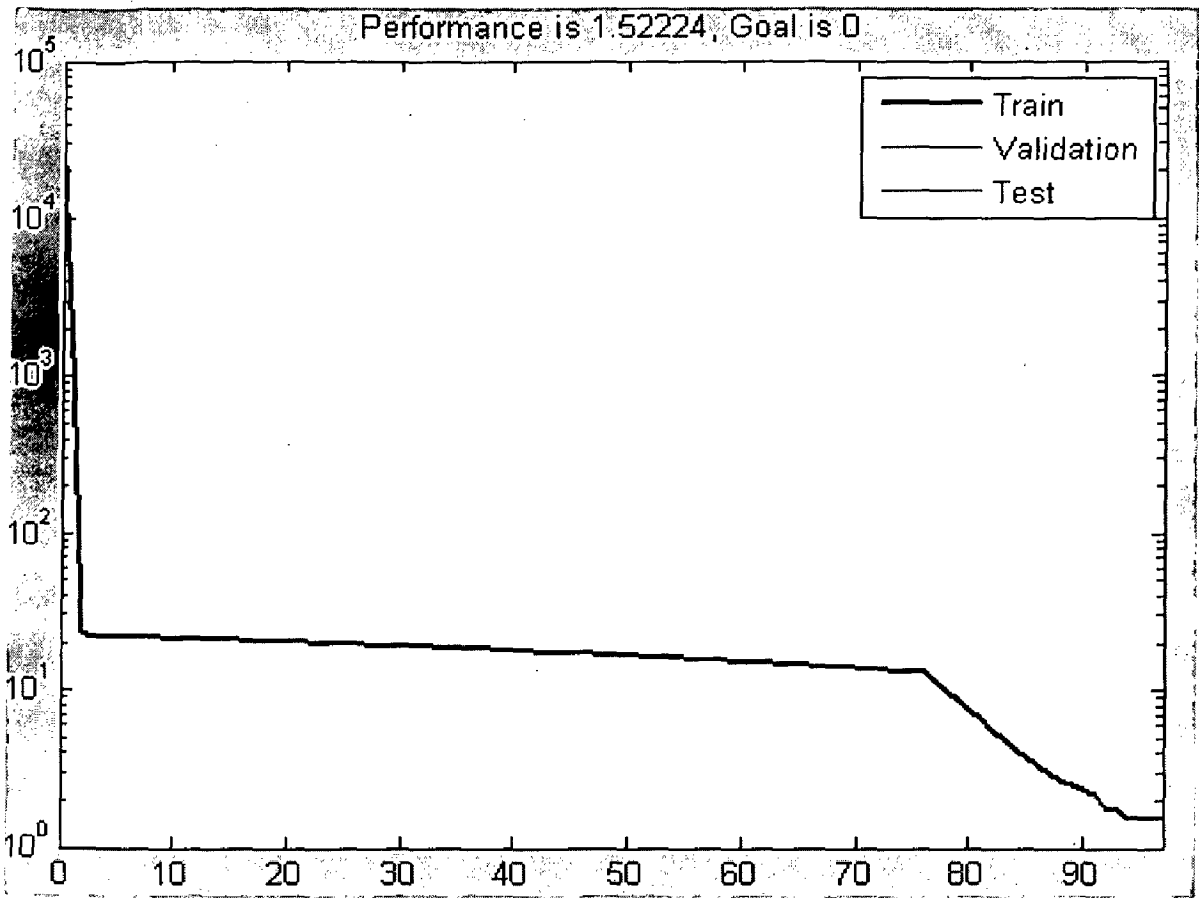


Figure 6.19 Training Curve for Model I

6.7.1.10 Model J

Figure 6.20 shows the structure of Model H as depicted in MATLAB Toolbox:

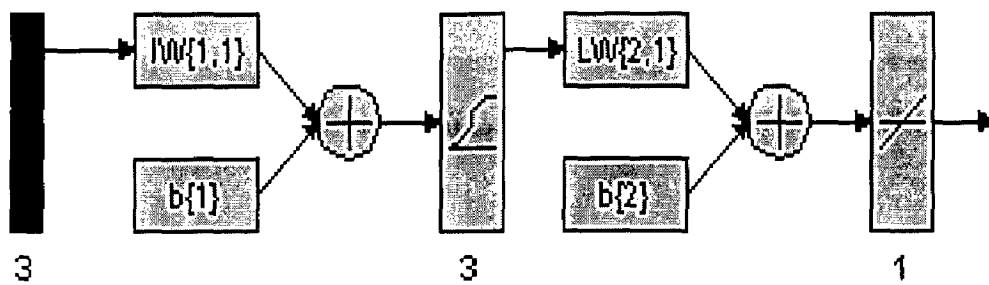


Figure 6.20: Layout of Model J

Training Curve for Model J is shown in Figure 6.21

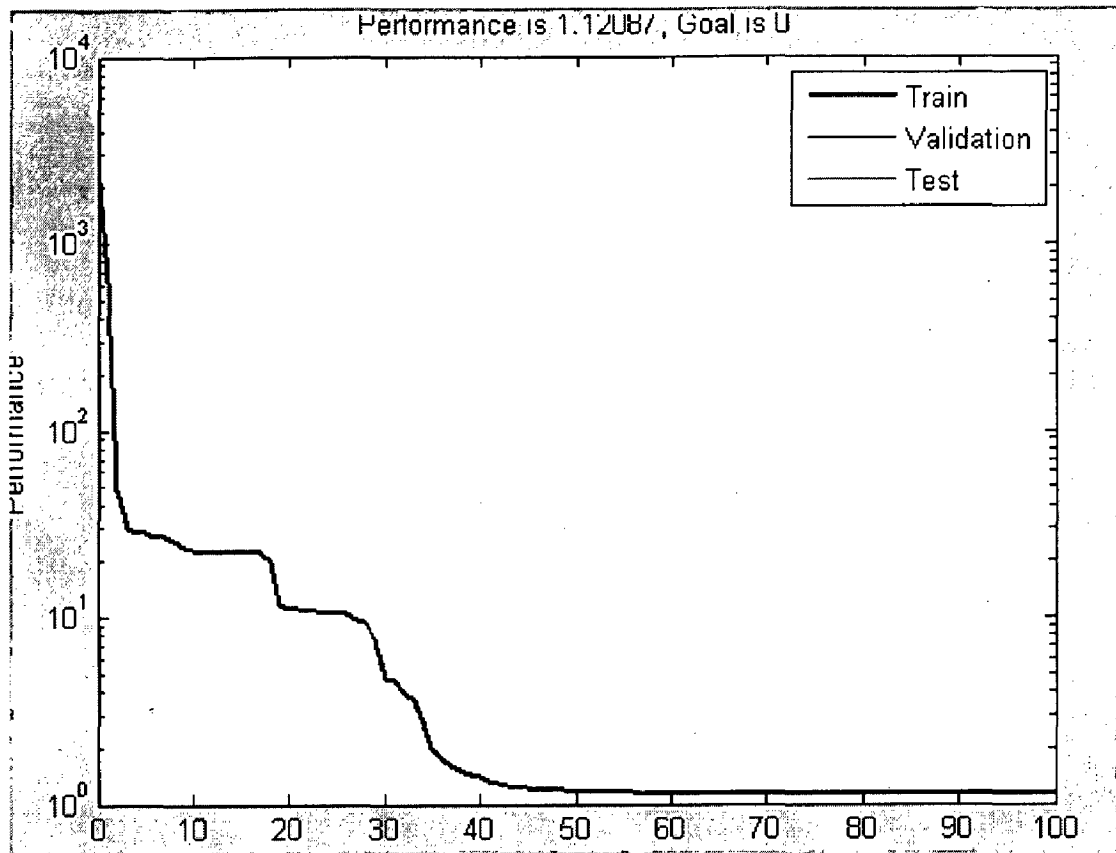


Figure 6.21 Training Curve for Model J

6.7.2 Discussion on the Training Trends of ANN Models

The ten models (Model A-Model J) as indicated above show diverse training features. In some models training was accomplished while in others, training was not successful. Therefore, we will consider only those models in which training was successful.

A summary is presented in Table 6.2 to provide an overview of the training results obtained.

The results show that only Models A, D, H, I and J could be trained. The rest i.e. Models B, C, E, F and G could not be trained with the activation functions and the hidden layer structure used. From above table we also observe that for same goal (zero) different activation functions give different performance in regard to convergence in terms of no. of epochs. Our main aim is to select an ANN model which gives less error i.e. output is nearer to the target value.

Here, **Model A** gives best results as compared to others; hence it is best model out of them. Now this model is used for simulation studies pertaining to pollution flashover in insulators.

Table 6.2 Summary of Training Results

S.No.	Model	target performance	goal	No. of epochs	Remarks
1	A	1.19651	0	51	Training accomplished
2	B	2033.46	0	1	Not trained
3	C	2033.46	0	1	Not trained
4	D	1.52224	0	47	Training accomplished
5	E	2033.46	0	1	Not trained
6	F	29.2538	0	11	Not trained
7	G	2033.46	0	2	Not trained
8	H	1.19651	0	60	Training accomplished
9	I	1.52224	0	97	Training accomplished
10	J	1.12087	0	100	Training accomplished

6.8 Verification of Accuracy of ANN models

Table 6.2 and Figure 6.22 show the results for the actual and predicted values of the selected ANN model (**Model A**)

Table 6.3 Analytical Values of FOV obtained using Model A

S. No.	Actual experimental Value of FOV (kV)	Predicted Value of FOV (kV)
1	60	60.1601
2	29	30.4334
3	47	46.7384
4	34	33.8347
5	38	38.9772

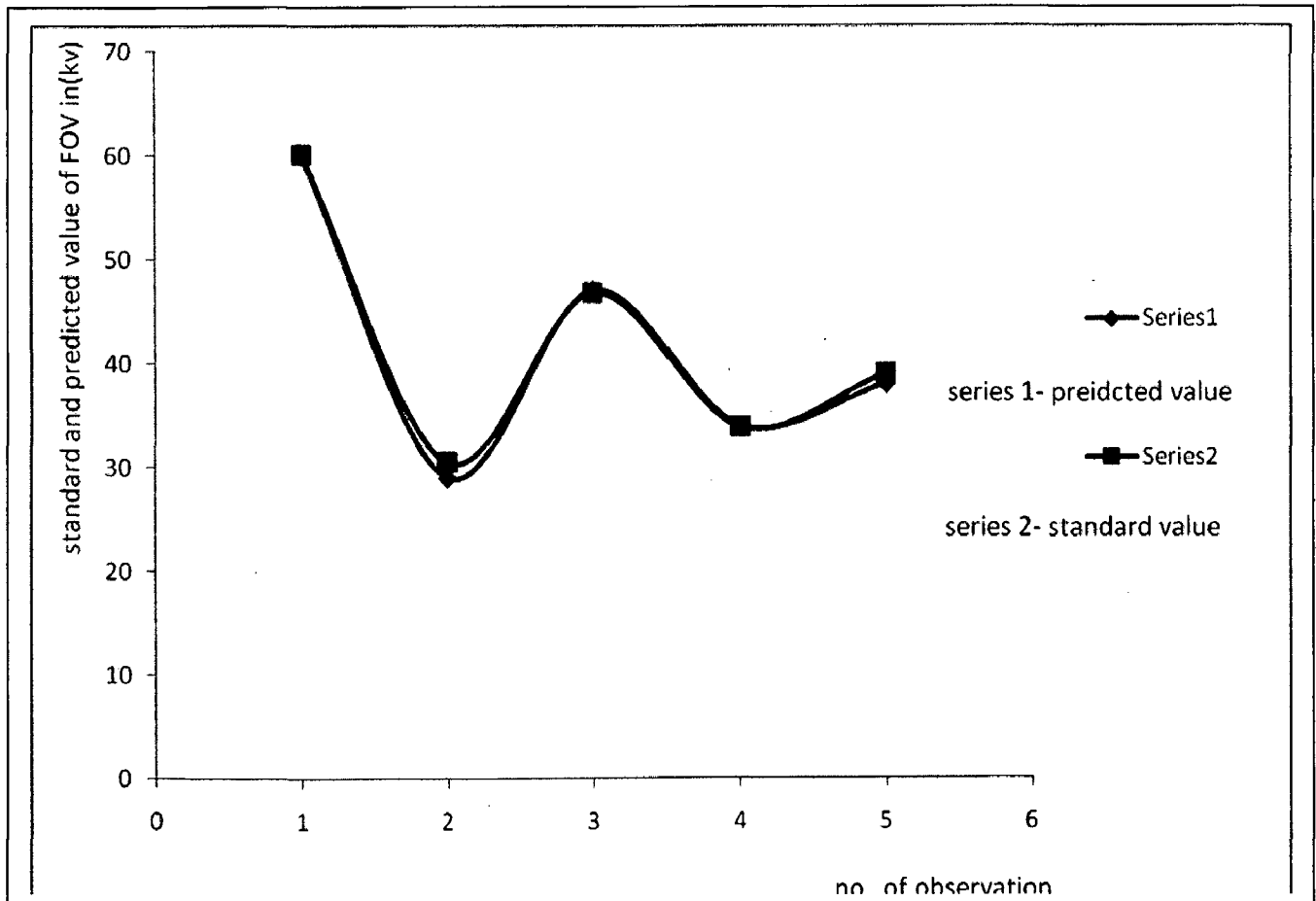


Figure 6.22 Graphical validation of Accuracy of ANN Model A

6.9 Summary

The present chapter is devoted to the evaluation and selection of a suitable ANN Model for predicting FOV of polluted insulators. Out of the ten models, **Model A** appeared to be the best. Hence its use is recommended for further simulation work.

CONCLUSIONS

7.1 Summary

The presented study was devoted to the evaluation and selection of a suitable ANN Model for predicting FOV of polluted insulators in terms of the input parameters viz. salinity, resistivity and current flow through the solution of the pollutant. Ten models (Model A –Model J), having different combinations of architectures and different activation functions with hidden and output layers were tried out. It was seen the best performance in terms of the goal attainment and the no. of epochs for convergence was shown by Model A. Hence this model is selected for subsequent simulation studies in relation to pollution flashover in polluted insulators.

7.2 Scope for Further Work

The present studies can be extended in the following ways:

- (a) Other method of analysis can be used e.g. Fuzzy based models, Fuzzy-neuro models, regression techniques, etc
- (b) Optimization of the parameters may be done to find out the best dimensions of the insulators to withstand flashovers for different levels of voltages.
- (c) Apart from the three control parameters (as used here), the use of other parameters can be investigated in enhancing the ANN model.
- (d) The studies have been restricted to flashover under AC voltages. The performance under High DC voltages can also be explored.

REFERENCES

- [1]. Farouk A.M. Rizk, Ahmed A. El-Sarky, Atared A. Assaad & Mohamed M. Awad, "Comparative Test on Contaminated Insulator with Reference to Desert Condition", CIGRE Report group 33-03, Vol.2, 1972 pages 1-9.
- [2]. Abdel-Salam H.A. Hamza, Nagat M.K. Abselgawad, Bahaa A. Arafa, "Effect of Desert Environmental Conditions on the Flashover Voltage of Insulators", Energy conversion and management 43 (2002), pages 2437-2442
- [3]. Patni, Prem K., "Review of Models which Predict the Flashover Voltage of Polluted Insulators", Ph.D thesis university of Monitoba Winnipeg, Monotoba, June 1997.
- [4]. W.Heise, G.F. Luxa, G.Revery and M.P. Verma (Germany) "Assessment of Solid Layer Artificial Pollution Test" CIGRE Report (33-09) volume -2 (1972), pages 1-11.
- [5]. Sundrarajan R. and Gorur R.S., "Role of Non Soluble Contaminants on the Flashover Porcelain Insulators", IEEE Transaction on Dielectric and Electrical Insulation, volume -3, No.1, February 1996, pages 113-118.
- [6]. Sundrarajan R. and Gorur R.S., "Effect of Insulator Profile on DC Flashover Voltage under Polluted Condition: a Study Using a Dynamic Arc Model", IEEE Transaction on Dielectric and Electrical Insulation, Volume No. 1 February 1994, pages 124-132.
- [7]. Raghuvver M.R. and E. Kuffel, "Experimental and Analytical Studies of Factor which Affect Pollution Flashover Voltage on Polluted Insulation Surfaces", IEEE Transaction on Power Apparatus and System, Vol. 74, January/February 1974, pages 312-320.
- [8]. Sundrarajan R. and Gorur R.S., "Dynamic Modeling of Flashover on Dielectric Surfaces" 3rd international conference on properties and application of dielectric materials, July 8-12, 1991 Tokyo, Japan
- [9]. Zafer Aydogmus and Mehmet Cebeci, "A New Flashover Dynamic Model of Polluted Insulators" IEEE Transaction and Electrical Insulation, Vol. 11, No. 4; August 2004 pages 577-583
- [10]. Holzhausen J.P. and Swift D.A. "Pollution Flashover of AC and DC Energized Cap and Pin Insulators: The Role of Shortening of the Arc", 4.333.p2
- [11]. Obenaus F., "Contamination Flashover and Creepage Path Length", ETZ 12, 1958 Pages 135-136
- [12]. Wilkins R., "Flashover Voltage of High Voltage Insulators with Uniform Surface Pollution Film" Proc. IEE, Vol. 116, No. 3, March 1969, Pages 457-465.

- [13]. Alston L.L. and Zoledziowski S., "Growth of Discharge on Polluted Insulation" Proc. IEEE, Vol.110, No.7, July 1963, Pages 1260-1266.
- [14]. Ahmad S., Ghosh, P.S., Shahnawaz Ahmad S. and Sayed Abdul Kader Aljunid, "Assessment of ESDD on High-Voltage Insulators Using Artificial Neural Network", Electric Power System Research Vol.72, June-2004, pages 131-136
- [15] Dixit, Pradeep Kumar and Gopal, H.G. "ANN Based 3- Stage Classification of the Arc Gradient of Contaminated Porcelain Insulators" 2004 International Conference on Solid Dielectrics , Toulouse, France, July 5-9, 2004.
- [16] Kontargyri V.T ,Gadketsi, A.A. Toekouras, G.J. Gorios. L.F. and Stathopulos. I.A. " Design of an Artificial Neural Network for the Estimation of Flashover Voltage on Insulators" Electrical Power System Research (Elsevier), Vol. 77 , 2007 pp. 1532-1540.
- [17] Ghosh, P.S. Chakravorti, S. and Chatterjee, N. " Estimation of Time to Flashover Characteristics of Contaminated Electrolytic Surfaces using Artificial Neural Network" IEEE Trans on Dielectrics & Electric Insulation 2 , 1995 pp 1064-1074.
- [18] Al-Alawi, S,Salam, M.A , Maqrashi, A.A. and Ahmed H "Prediction of Flashover Voltage of Contaminated Insulator Using Artificial Neural Network": Electrical Power Components and Systems, Vol. 34 pp 831-840, 2006
- [19]. Tsanakas A.D. and Agoris D.P., "Pollution Flashover Fault Analysis and Forecasting Using Neural Network". CIGRE Report 2002, University of Patras (Greece)
- [20] "Automated Operating Procedures for Transfer Limits" Report of Power System Engg. Research Centre, Washington State University, USA, May 2001 (PSERC Publication 01-05)